

REVIEW ARTICLE

Multi-Valued Solution and Level Set Methods in Computational High Frequency Wave Propagation

Hailiang Liu^{1,*}, Stanley Osher² and Richard Tsai³

¹ *Department of Mathematics, Iowa State University, Ames, IA 50011, USA.*

² *Level Set Systems, Inc, 1058 Embury Street, Pacific Palisades, CA 90272-2501, USA.*

³ *Department of Mathematics, University of Texas, Austin, TX 78712, USA.*

Received 28 April 2006; Accepted (in revised version) 24 May 2006

Abstract. We review the level set methods for computing multi-valued solutions to a class of nonlinear first order partial differential equations, including Hamilton-Jacobi equations, quasi-linear hyperbolic equations, and conservative transport equations with multi-valued transport speeds. The multivalued solutions are embedded as the zeros of a set of scalar functions that solve the initial value problems of a time dependent partial differential equation in an augmented space. We discuss the essential ideas behind the techniques, the coupling of these techniques to the projection of the interaction of zero level sets and a collection of applications including the computation of the semiclassical limit for Schrödinger equations and the high frequency geometrical optics limits of linear wave equations.

Key words: Multi-valued solution; level set method; high frequency wave propagation.

Contents

1	Introduction	766
2	Level set framework for first order equations	770
3	Semiclassical approximations	777
4	WKB approximation	779
5	General symmetric hyperbolic systems	788
6	Numerical examples	793
7	Conclusions	798

*Correspondence to: Hailiang Liu, Department of Mathematics, Iowa State University, Ames, IA 50011, USA. Email: hliu@iastate.edu

1 Introduction

In the computation of wave propagation, when the wave field is highly oscillatory, direct numerical simulation of the wave dynamics can be prohibitively costly and approximate models for wave propagation must be used. The resulting approximate models are often nonlinear, and the corresponding classical entropy or viscosity type solutions are not adequate in describing the wave behavior beyond the singularity, where multi-valued solutions in physical space are needed. Therefore, capturing multi-valued solutions by efficient algorithms is an important issue. Examples include dispersive waves [30, 40, 62], optical waves [17, 18], seismic waves [23, 57, 61], semiclassical limits of Schrödinger equations [10, 33, 56], electron beam modulation in vacuum electronic devices [41], etc. More applications arise constantly.

The level set method has been a highly successful computational technique for capturing the evolution of curves and surfaces [49, 50] with applications in diverse areas such as multi-phase fluids, computer vision, imaging processing, optimal shape design, etc. This paper reviews a newly developed level set framework for the computation of multi-valued solutions of a large class of nonlinear PDEs that are encountered in various high frequency wave propagation problems mentioned above. We hope that this article will help the community understand how ideas of the level set method have been used in this challenging area, and the problems that remain in extending this method to other physical applications.

1.1 Asymptotic methods

We consider a complex wave field $u^\epsilon(x, t)$ governed by a linear wave type equation, say the Schrödinger equation

$$i\epsilon u_t^\epsilon = -\frac{\epsilon^2}{2}\Delta u^\epsilon + V(x)u^\epsilon,$$

where $V(x)$ is a given potential, and $\epsilon > 0$ denotes a re-scaled Planck constant. Here the regime of interest is the so called *semiclassical approximation* where ϵ tends to zero. A widely used classical approach is the so called WKB method or geometrical optics, which uses asymptotic approximations obtained when the small scale goes to zero.

The derivation of the WKB system comes through a formal expression

$$u^\epsilon(x, t) = A^\epsilon(x, t) \exp(iS(x, t)/\epsilon). \quad (1.1)$$

Assuming that the phase S and the amplitude A^ϵ are sufficiently smooth, we expand the amplitude in powers of ϵ :

$$A^\epsilon = A_0 + \epsilon A_1 + \epsilon^2 A_2 + \dots .$$

Insertion of this expression into the underlying linear wave equation and balancing terms of $\mathcal{O}(1)$ order in ϵ gives separate equations for A and S .

The phase will satisfy a nonlinear first order equation of Hamilton-Jacobi (HJ) type

$$S_t + H(x, \nabla_x S) = 0, \quad (1.2)$$

where $H(x, p)$ is a Hamiltonian. For instance, $H(x, p) = \frac{1}{2}|p|^2 + V(x)$ for the Schrödinger equation.

The leading order term in the amplitude, A_0 , solves a transport equation of the following form

$$\rho_t + \nabla_x(\rho \nabla_p H(x, \nabla_x S)) = 0, \quad (1.3)$$

where $\rho = A_0^2$. When ϵ is small, the leading term, A_0 , becomes significant.

The above system is only weakly coupled since the phase S solves the Hamilton-Jacobi equation that is independent of the amplitude. Instead of the oscillatory wave field, the unknowns in the WKB system are the phase S and the amplitude A_0 , neither of which depends on the small scale. Hence they are usually easier to compute numerically.

1.2 Multi-valued solutions

The solution of the Hamilton-Jacobi equation in general does not possess a superposition principle as the solution of the original linear wave equation does, and develops singularities in the derivatives in finite times. The so called viscosity solution can be used to define a notion of unique weak solution [14, 39]. However, this class of weak solutions is not adequate for treating dispersive wave propagation problems or solution to the wave equation because crossing wave fronts and superposition of solutions are important. Moreover, using the entropy or viscosity notion in solving the transport equation (1.3) may lead to a measure-valued solution. This means that the intensity A^2 may develop a Dirac delta function supported along the shock curves of the phase variable S . See e.g. [4, 7, 8, 15, 27, 54]. These singularities are called caustics and the energy of the wave becomes infinite there. This clearly contradicts the a priori estimates for the underlying linear wave equation.

A natural way to avoid such difficulties is to seek multi-valued phases corresponding to crossing waves. This means that in general for every non-caustic location in space and time, (x, t) , a set of phase functions $\{S_i\}$, $i = 1, 2, \dots$ is constructed. Each of these functions is a solution of the Hamilton-Jacobi equation in a neighborhood of (x, t) with suitable boundary conditions that couple them together. This set of solutions is referred to as the multi-valued solution of the Hamilton-Jacobi equation. Each S_i is called a branch of the multi-valued solution. In the context of wave propagation, each branch corresponds to an arrival of certain phases at that location while the viscosity solution picks out the phase corresponding to the first arrival wave.

1.3 Numerical methods

The classical way to compute the multi-phases is through Lagrangian methods (ray tracing). The ray equations are nothing but the characteristic system of the HJ equation

$$\frac{dx}{dt} = \nabla_p H(x, p), \quad \frac{dp}{dt} = -\nabla_x H(x, p), \quad (1.4)$$

where p is the momentum variable in phase space. The amplitude A_0 along the ray can also be computed via tracking the geometric spreading across the wave front:

$$q(t) := \text{Det} \frac{\partial x(t; x_0)}{\partial x_0},$$

where x_0 is the initial value of x for the ray equations. For scalar wave equations, the amplitude is related to q by

$$\frac{A_0^2(x(t))}{c^2(x(t))} q(t) = \frac{A_0^2(x(0))}{c(x(0))} q(0).$$

We can track $q(t)$ by evolving the dependence of the ray solution on the initial conditions x_0 , i.e., $\partial x(t; x_0)/\partial x_0$ and $\partial p(t; x_0)/\partial x_0$. Note that $p(0; x_0)$ describes the initial wave front geometry in the physical space.

This method is easy to implement, but has an obvious drawback which lies in numerically maintaining adequate spatial resolution of the wave front in regions with diverging rays. This problem is avoided in Eulerian methods, through the use of uniform grids in their computations, see, e.g., [2, 3]. As we mentioned in the previous section, Eulerian methods that are based on solving the HJ equation, however, have difficulties in handling the multi-valued solutions [16].

One approach for improving physical space-based Eulerian methods is the use of a kinetic formulation in the phase space (t, x, p) , in terms of a particle density function $w(t, x, p)$ that satisfies Liouville's equation

$$w_t + \nabla_p H \cdot \nabla_x f - \nabla_x H \cdot \nabla_p w = 0. \quad (1.5)$$

Such a formulation was first used in the context of multi-phase computation for optical waves [6, 17, 18].

A direct link between the above Liouville equation and the original wave field u^ϵ is in the scaled Wigner transform

$$w^\epsilon(t, x, p) = \left(\frac{1}{2\pi} \right)^d \int e^{ip \cdot y} u^\epsilon(t, x - \epsilon y/2) \bar{u}^\epsilon(x + \epsilon y/2) dy, \quad (1.6)$$

where \bar{u} is the conjugate of u . The Wigner function $w(t, x, p)$ is not necessarily positive. It becomes positive in the limit $\epsilon \rightarrow 0$. Moreover, it has the property

$$\int w^\epsilon(t, x, p) dp = u^\epsilon(t, x) \bar{u}^\epsilon(t, x). \quad (1.7)$$

The limiting equation for w when $\epsilon \rightarrow 0$ leads to the above Liouville equation (1.5). Wigner transform has been widely used in the study of high frequency, homogenization limits of various equations, see e.g., [24, 32, 42, 53, 56]. The limit w of w^ϵ is a locally bounded nonnegative measure and for the WKB form of solution we have

$$w(t, x, p) = A^2(t, x) \delta(p - \nabla_x S),$$

from which it follows that the amplitude at a point x is given as the integral of w over the phase variable,

$$A^2(t, x) = \int w(t, x, p) dp.$$

The support of w corresponds to the wave front. The Wigner transformation provides a phase space description of the equations of the problem and has been shown to be very useful for asymptotics since it “unfolds” the caustics, due to the linearity of the Liouville equation in phase space. This technique provides an alternate approach to the WKB method, see, e.g., [56]. There is, however, a serious drawback with direct numerical approximations of the Liouville equation which is the need for a large set of independent variables in the phase space. There are two ways to remedy this problem which are suggested in the literature. One is the moment method, which is based on reducing the number of independent variables by introducing equations for moments, see [5, 6, 17, 26, 28, 33]. The other is based on computations of special wave front solutions. For tracking wave fronts in geometric optics, geometry based methods in phase space such as the segment projection method [19] and the level set method [10, 11, 48, 51] have been recently introduced. Consult [18] for a recent survey on computational high-frequency wave propagation.

Recently a geometric viewpoint has been adopted in place of the kinetic one in phase space. With this new viewpoint a new level set method framework has been developed for computing multi-valued phases and other physical observables in the entire physical domain in [10, 34–36, 43].

A key idea in [10, 36, 43] is to represent the n -dimensional bi-characteristic manifold of the Hamiltonian-Jacobi equation in phase space by an implicit vector level set function $\phi(t, x, p)$, whose components solves the same Liouville equation

$$u_t + \nabla_p H \cdot \nabla_x u - \nabla_x H \cdot \nabla_p u = 0. \quad (1.8)$$

The multi-valued phase gradient, $\nabla_x S$, is realized by the zero level set

$$\phi(t, x, p) = 0.$$

The multi-valued function S can be resolved on the entire physical domain by the intersection of $n + 1$ zero level sets in the jet space (x, p, z) through solving $n + 1$ level set equations [10, 43].

Based on the level set framework in the phase space, the amplitude is evaluated:

$$\rho(t, x) = \int f(t, x, p) \delta(\phi) dp,$$

where the quantity f also solves the same Liouville equation $\phi = 0$ but with initial density $\rho(x, 0)$ as initial data. The multi-valued higher moments can be also resolved by integrating f along the bi-characteristic manifold in the phase directions, see [34, 35].

The main advantages of these new approaches, in contrast to the standard kinetic approach using the Liouville equation with a Dirac measure initial data, include: 1) the Liouville equations are solved with L^∞ initial data, and a singular integral involving the Dirac- δ function is evaluated only in the post-processing step, thus avoiding oscillations and excessive numerical smearing; 2) a local level set method can be utilized to significantly reduce the computation cost in the phase space. These methods can be used to compute *all* physical observables for multidimensional problems.

In computing the level set equation in phase space, since the area of interest is close to the zero level set, it is possible to use fast local level set techniques in the same manner as in, e.g., [10, 11, 48, 51], which will reduce the computational cost and also reduce the storage requirements [46]. Recently, Cheng proposed what appear to be a very efficient semi-Lagrangian method that is specialized for the phase space level set calculation on adaptive grids [9].

In this paper we shall mainly focus on various level set formulations and associated numerical techniques applied to several important wave equations. Section 2 is devoted to the level set framework in both phase space and jet space for general first-order PDEs. We shall mainly follow the presentation in [10, 43], in which a level set framework is set up for capturing both velocity and the phase S , as well as multi-valued solutions for very general first order PDEs. In Section 3 we discuss the computation of the semiclassical limit, adapted from [35]. Section 4 is devoted to more general WKB system and applications to symmetric hyperbolic wave equations, following [34]. We refer to [10, 34–36, 43] for various numerical examples. Finally we give a summary and point out some new directions of research.

2 Level set framework for first order equations

2.1 Level set framework for graph evolution

We start with a scalar conservation law of the form

$$u_t + \nabla_x \cdot F(u) = 0, \quad u(x, 0) = g(x).$$

Singularities in the derivatives of solutions will generally develop in finite time even for a large class of very smooth initial values. This happens when characteristics collide at a physical location. After the occurrence of each singularity, the entropy solution is often chosen to capture the physically relevant solution in applications such as gas dynamics. However, when we regard the characteristics equations as a system of ordinary differential equations in its configuration space, we see that the existence of the ODE solutions suggests multi-valued solutions beyond the collision of characteristic curves.

In fact, the multi-valued nature of this problem can be seen from the following implicit formula for the solution

$$u(x, t) = g(x - F'(u)t);$$

when $\nabla_x g \cdot F''(u) < 0$, it is possible to have more than one solution at each (x, t) .

To track a multi-valued solution, we may simply evolve the graph of $u(x, t)$ as a surface in the (x, p) space by a velocity field prescribed by the characteristics. In this way, the above implicit function is equivalent to the level set formulation

$$\phi(t, x, p) = 0, \quad \phi := p - g(x - F'(p)t).$$

This implicit representation is still valid beyond the crossing of characteristics. We can easily derive the evolution equation for ϕ in the phase space (x, p) :

$$\partial_t \phi + F'(p) \cdot \nabla_x \phi = 0,$$

subject to the initial data

$$\phi(0, x, p) = p - g(x).$$

We can thus capture the multi-valued solution of the above quasi-linear equation by solving the level set equation followed by a post-projection procedure

$$(x, u) \in \{(x, p) \mid \phi(t, x, p) = 0\}.$$

Such a level set formulation based on the graph evolution can be traced back to Jacobi (who did not consider multi-valued solutions), and has been extensively used in various contexts, see e.g. [13,21,25,47,60]. These earlier works focused either on the solution before the formation of multiple values or on preventing multi-valued solutions. In [10,36], the level set formulation was first used as a numerical device to capture multi-valued solutions for general quasilinear hyperbolic equations

$$\partial_t u + F(u, x) \cdot \nabla_x u = B(u, x).$$

The corresponding level set equation is

$$\partial_t \phi + F(z, x) \cdot \nabla_x \phi + B(z, x) \partial_z \phi = 0.$$

It is tempting to try this same idea for the Hamilton-Jacobi equation

$$\partial_t S + H(x, \nabla_x S) = 0.$$

That is, let the solution S be realized by an implicit relation

$$\phi(t, x, z) = 0, \quad z = S(x, t).$$

Differentiation in both x and t leads to

$$\partial_t S = -\frac{\phi_t}{\phi_z}, \quad \nabla_x S = -\frac{\nabla_x \phi}{\phi_z}.$$

The equation for ϕ can be formally written as

$$\phi_t - H\left(x, -\frac{\nabla_x \phi}{\phi_z}\right) \phi_z = 0.$$

However, unless $H(x, p)$ is linear in p , this nonlinear formulation is not appropriate for computing multi-valued solution S . To unfold the singularity caused by nonlinearity in p , one has to add $p = \nabla_x S$ into the configuration space.

Following [43] we present a systematic level set framework in the jet space for general first order PDEs.

2.2 Level set formulation in jet space

We consider a general first-order nonlinear equation

$$G(\xi, u, \nabla_\xi u) = 0, \quad (2.1)$$

where $G : (\xi, z, q) \in \mathbb{R}^m \times \mathbb{R} \times \mathbb{R}^m \rightarrow \mathbb{R}$ is a smooth function, $u \in \mathbb{R}$ is the unknown function of $\xi \in \mathbb{R}^m$. Furthermore, $G(\xi, z, q)$ satisfies the non-degeneracy assumption

$$|\nabla_q G(\xi, z, q)|^2 \neq 0,$$

which ensures that (2.1) is a first order equation.

Following [10, 43], we introduce a generic level set function $\phi(\xi, z, q)$ in an extended space $(\xi, z, q) \in \mathbb{R}^{2m+1}$ so that the solution $z = u(\xi)$, and also its gradient $\nabla_\xi u$, stay on the zero level set

$$\phi(\xi, z, q) = 0, \quad z = u(\xi), \quad q = \nabla_\xi u(\xi).$$

Under the usual regularity assumptions on G and the initial data, the characteristics of (2.1) exists at least locally. Let such characteristics be parameterized as $(\xi, z, q) = (\xi, z, q)(\tau)$. The level set function should be independent of the parameter τ . Therefore,

$$\frac{d}{d\tau} \phi(\xi(\tau), z(\tau), q(\tau)) \equiv 0,$$

which gives the level set equation

$$\vec{A} \cdot \nabla_{\{\xi, z, q\}} \phi = 0,$$

where $\vec{A} := \left(\frac{d\xi}{d\tau}, \frac{dz}{d\tau}, \frac{dq}{d\tau}\right)$ denotes the direction field of the characteristics. According to the classical theory of characteristics for general differential equations of the first order, see [13, page142-144], the vector field is determined by

$$A_1 = \nabla_q G, \quad A_2 = q \cdot \nabla_q G, \quad A_3 = -\nabla_\xi G - q \cdot \partial_z G.$$

Thus the level set equation is

$$\nabla_q G \cdot \nabla_\xi \phi + q \cdot \nabla_q G \partial_z \phi - (\nabla_\xi G + q \partial_z G) \cdot \nabla_q \phi = 0, \quad (2.2)$$

which, as a linear homogeneous equation, serves to ‘unfold’ multi-valued quantities wherever they occur in the physical space. The level set equation in such generality can be used to capture characteristics systems of the problem, including the bi-characteristics strips, the solution value u and its gradient ∇u .

The construction of the level set functions ϕ at initial time is dependent on the specific details of each problem, and we shall discuss this issue in each specific problem that we discuss.

In the following, we review two common types of problems that can be solved by the Jet Space Level Set Formulation.

2.2.1 Level set formulation for quasi-linear transport equations

Consider the first-order time-dependent transport equation:

$$\partial_t u + F(u, x, t) \cdot \nabla_x u = B(u, x, t), \quad x \in \mathbb{R}^n, \quad u \in \mathbb{R}^1. \tag{2.3}$$

Take $\xi = (t, x)$ and $q = (p_0, p)$ with $p_0 = \partial_t u$, $p := \nabla_x u$, and the equation (2.3) can be rewritten as $G = 0$ where

$$G := p_0 + F(z, x, t) \cdot p - B(z, x, t), \quad z = u.$$

A simple calculation gives

$$\nabla_q G \cdot \nabla_\xi \phi = \partial_t \phi + F(z, x, t) \cdot \nabla_x \phi$$

and

$$q \cdot \nabla_q G \phi_z = (1, F) \cdot (p_0, p) = p_0 + F \cdot p = B(z, x, t) \phi_z,$$

where we use the fact $G = p_0 + F \cdot p - B = 0$. The level set equation (2.2) in this setting reduces to

$$\partial_t \phi + F \cdot \nabla_x \phi + B \partial_z \phi + A_3 \cdot \nabla_q \phi = 0,$$

where

$$A_3 = (-\partial_t G - p_0 \partial_z G, -\nabla_x G - p \partial_z G).$$

Note that the transport speeds in the x and z -directions do not explicitly depend on (p_0, p) . Therefore, the level set function will not depend on $q = (p_0, p)$ if it does not do so initially. Thus, the effective level set equation in the phase space (t, x, z) reads as

$$\partial_t \phi + F \cdot \nabla_x \phi + B \partial_z \phi = 0. \tag{2.4}$$

With the initial data

$$\phi(0, x, z) = z - u_0(x),$$

the solution u to (2.3) can be determined as the zero level set,

$$u \in \{z, \quad \phi(t, x, z) = 0\}.$$

In this case, we only need one level set function ϕ . Here the level set $\phi(t, x, u) = 0$ can be regarded as a complete integral to (2.4), which implicitly determines u , see [13, page 140].

2.2.2 Level set formulation for Hamilton-Jacobi equations

Consider a generalized Hamilton-Jacobi equation

$$\partial_t S + H(x, S, \nabla_x S) = 0. \quad (2.5)$$

Note that classically, Hamilton-Jacobi equations refer to the ones for which H is a Hamiltonian function and is independent of the solution S . However, in literatures, equation of the form (2.5) is also called the same name. Here, we call it a generalized Hamilton-Jacobi equation to distinguish it from the classical case. The dependence of S fundamentally changes the behavior of the solution.

Since the generalized Hamiltonian $H(x, z, p)$ may be nonlinear in all its arguments, we need to develop the level set formulation in the jet space, with t as a marching parameter.

A straightforward calculation based on the above gives an effective level set equation for (2.5)

$$\partial_t \phi + \nabla_p H \cdot \nabla_x \phi + (p \cdot \nabla_p H - H) \partial_z \phi - (\nabla_x H + p H_z) \cdot \nabla_p \phi = 0, \quad (2.6)$$

where $\phi := \phi(t, x, z, p)$ is well defined in the space $(x, z, p) \in \mathbb{R}^{2n+1}$ for fixed t . We need $n + 1$ independent level set functions in this case. Their common zero level set captures the desired solution in phase space.

If the Hamiltonian H does not depend explicitly on S , i.e., $H_z = 0$, (2.6) will lead to the level set equation in phase space

$$\partial_t \phi + \nabla_p H \cdot \nabla_x \phi + (p \cdot \nabla_p H - H) \partial_z \phi - \nabla_x H \cdot \nabla_p \phi = 0. \quad (2.7)$$

Note that when H does not depend on z explicitly, the level set function ϕ will be independent of z , if it is chosen so initially. Therefore, if one just wants to capture the wave front or resolve the gradient of S , the effective level set equation reduces to

$$\partial_t \phi + \nabla_p H \cdot \nabla_x \phi - \nabla_x H \cdot \nabla_p \phi = 0. \quad (2.8)$$

This is the well-known Liouville equation. In this case, n independent level set functions are needed.

Finally, the initial data for equation (2.7) can simply be chosen as

$$\begin{aligned} \phi_1(0, x, z, p) &= z - S_0(x), \\ \phi_i(0, x, z, p) &= p_i - \partial_{x_i} S_0(x), \quad i = 2, 3, \dots, n + 1. \end{aligned}$$

In the case of equation (2.8), ϕ_1 is not needed.

2.3 Numerical implementation

Let us illustrate this by an example of equation (2.8) in \mathbb{R}^2 with the inhomogeneous Hamiltonian $H(x, p) = (p^2 + x^2)/2$. This is a Hamiltonian flow and the total energy $H(x(t), p(t))$ is invariant under the flow. More precisely, for $t \geq 0$, $(x(t), p(t))$ stays on the invariant manifold \mathcal{M}_0 , which is the H_0 level set of the Hamiltonian H determined by the initial data (x_0, p_0) . Furthermore, since the Hamiltonian is unbounded at infinity, \mathcal{M}_0 is a bounded closed submanifold in the phase space. Hence, the range of (x, p) is determined by the given initial data and the Hamiltonian.

With the initial data $(x_0, p_0) = (\sqrt{2}, \sqrt{2})$, the invariant manifold $\mathcal{M}_{\sqrt{2}}$ is the two-level set of H , corresponding to the circle with radius two, centered at the origin. Therefore, the possible range of p for this system is bounded by the extrema of p constraint on the circle; in this example it is $[-2, 2]$. Correspondingly, we can determine the range of x . Of course, for our problem, we generally evaluate a system of such flows determined by $(x, \partial_x S_0(x))$, with $x \in \Omega_x$ and Ω_x compact. We then determine the range of (x, p) needed for computation by obtaining bounds determined from each energy level set $\mathcal{M}_x, x \in \Omega_x$.

We implement the level set method for computing multi-valued velocity fields. Our algorithm for computing the velocity can be summarized as follows.

1. Initialize: construct the level set functions $\Phi_0 = (\phi_j^{(0)})$ that embed the initial data $\nabla_{\mathbf{x}} S_0$,

$$\phi_j^{(0)}(\mathbf{x}, \mathbf{k}) = k_j - \frac{\partial}{\partial x_j} S_0(\mathbf{x}), \quad j = 1, \dots, n.$$

2. Evolve the Liouville equation in phase space using $\phi_j^{(0)}$ constructed above as initial conditions:

$$\begin{aligned} w_t + \nabla_{\mathbf{k}} H \cdot \nabla_{\mathbf{x}} w - \nabla_{\mathbf{x}} H \cdot \nabla_{\mathbf{k}} w &= 0, \\ w(0, x, p) &= \phi_j^{(0)}, \quad j = 1, \dots, n. \end{aligned}$$

3. Realize the multi-valued velocity by projection onto the common zero sets of level set functions $\phi_j(t, x, p)$, i.e.,

$$u \in \bigcap_{j=1}^n \{p, \quad \phi_j(t, x, p) = 0\}.$$

We suggest some guiding principles for designing a level set algorithm for multivalued solutions, following [43]:

- When implementing the level set method, reducing to a lower dimension is preferred in order to lower the computational cost. In general such a reduction is indeed possible if the variables in the lower dimension give us the quantities we want to compute and these variables independently evolve along the characteristic field in the full space (ξ, z, q) .

- If the reduced space dimension is m and the object of interest is k dimensional, then we use $m - k$ level set functions.
- The initial data should be chosen in such a way that the interaction of zero level sets of these chosen initial data uniquely embeds the given initial data in the original PDE problem.

Consult [10, 36] for more implementation details and numerical examples. We also refer to [43] for numerical procedures of computing multi-valued phase S as well as multi-valued solutions to general first order PDEs.

So far, most of the published work in computing multi-valued solutions using the level set method deal with either classical Hamilton-Jacobi equations or linear Schrödinger equations. The corresponding phase space equations are the Liouville equations in two to six dimensions, depending on the dimension of the original wave equations. What is special about the level set formulations discussed above is that only the lower dimensional Lagrangian manifolds are of real interests, as they describe the propagation of the wave fronts and the energy. Due to the nature of convection, the evolution of a non-characteristics data set is dependant only on itself. Therefore, conventional local level set techniques can be combined with high resolution WENO discretizations for the partial derivatives and a Runge-Kutta time step discretization to compute the evolution. Notice that forward Euler in time together with 5th order WENO discretization does not yield stable numerical schemes. An interesting approach using spectral and discontinuous Galerkin methods can be found in [12].

Recently, there have developed several numerical approaches that are specialized for phase space calculations. These approaches adopted semi-Lagrangian methods that can be derived by back-tracing characteristics from each grid node. In general, semi-Lagrangian methods have the flexibility of handling non-regular grid geometries as long as suitable interpolation algorithms exist for the particular grid structure. Hence, a fine grid concentrating at the zeros of the level set functions can be created to maintain uniform resolution at all time. See [9, 52].

When computing the Liouville equation with discontinuous Hamiltonian in spatial variables, one encounters additional difficulties. The simplest case is the transmission problem for optical waves [11]. Some numerical techniques have been recently introduced by Jin et al [37, 38], so that the Hamiltonian is still preserved after crossing discontinuities.

Depending on the phase space that is adopted, appropriate boundary conditions should be imposed on the computation boundaries so that the problem is well-posed and no artificial and spurious wave fronts are generated and propagated into the computational domain. If the entire wave fronts are contained in the computational domain, Neumann boundary conditions can be used at the computation boundaries. In certain situations when the computational domain covers only a portion of a closed wave front, Neumann conditions might not be suitable since it may alter the geometry of the wave fronts. Please see [48] for some examples in geometrical optics.

3 Semiclassical approximations

We now turn to applications of level set methods introduced previously. Consider the linear Schrödinger equation

$$i\epsilon\partial_t\psi^\epsilon = -\frac{\epsilon^2}{2}\Delta\psi^\epsilon + V(x)\psi^\epsilon, \quad x \in \mathbb{R}^n, \quad (3.1)$$

subject to a highly oscillatory initial wave function

$$\psi(x, 0) = A_0(x) \exp(iS_0(x)/\epsilon), \quad (3.2)$$

where V is a given smooth potential, and ϵ is the scaled Planck constant. In the semiclassical regime which corresponds to a small value ϵ , the wave field ψ^ϵ and its associated physical observables become highly oscillatory within the wave length $O(\epsilon)$, directly, and thus numerical simulation of the wave field becomes very costly. A natural way to remedy this problem is to use some approximate models which can resolve the small-scale in the wave field. The classical approach is the WKB method, which are asymptotic approximations obtained as the small scale goes to zero. The WKB (Wentzel-Kramers-Brillouin) ansatz consists of representing the wave field function ψ^ϵ in the form

$$\psi^\epsilon(x, t) = A^\epsilon(x, t) \exp(iS(x, t)/\epsilon), \quad A^\epsilon(x, t) = \sum_{j=0}^{\infty} \epsilon^j A_j(x, t). \quad (3.3)$$

With this decomposition, the most singular part of the wave field is characterized by two quantities, the phase function S which satisfies a nonlinear eikonal equation and the amplitude function A which, to leading order, satisfies a transport equation, i.e.,

$$\partial_t S + \frac{|\nabla_x S|^2}{2} + V(x) = 0, \quad (3.4)$$

$$\partial_t A_0^2 + \nabla_x \cdot (A_0^2 \nabla_x S) = 0. \quad (3.5)$$

This is a weakly coupled system which means that one could solve the phase S independent of the position density $\rho = |A_0|^2$.

3.1 Phase and velocity

The phase equation (3.4) is a Hamilton-Jacobi equation of the form

$$\partial_t S + H(x, \nabla_x S) = 0, \quad x \in \mathbb{R}^n, \quad (3.6)$$

with $H(x, p) = |p|^2/2 + V(x)$. In [10] the authors introduced a systematic level set framework to compute the multi-valued solutions to Hamilton-Jacobi equations. The phase gradient is implicitly embedded into a n -dimensional manifold, which is the intersection of zero sets of n level set functions, each satisfying the Liouville equation

$$\partial_t \phi + p \cdot \nabla_x \phi - \nabla_x V \cdot \nabla_p \phi = 0. \quad (3.7)$$

This also gives the multi-valued solution to the equation

$$\partial_t u + u \cdot \nabla_x u = -\nabla_x V, \quad (3.8)$$

which is formally the gradient of the Hamilton-Jacobi equation (3.6). Here $u = \nabla_x S$ is the phase gradient and can be regarded as the corresponding velocity. The averaged velocity will be evaluated via the formula (3.14).

As pointed in [10], the equation (3.7) in phase space is not enough to resolve the phase S ; an additional level set function in the augmented space (x, p, z) with $z = S(x, t)$ is used in [10] to resolve the multi-valued phase. More precisely, the multi-valued phase is captured by solving the level set equation, a special case of (2.7):

$$\partial_t \phi + p \cdot \nabla_x \phi + \left(\frac{|p|^2}{2} - V(x) \right) \partial_z \phi - \nabla_x V \cdot \nabla_p \phi = 0, \quad (3.9)$$

subject to initial data $\phi(0, x, z, p) = (p - \nabla_x S_0(x), z - S_0(x))^T$. The intersection of components of the obtained vector level set function gives the co-dimensional n object.

3.2 Density evaluation

With the obtained phase and phase gradient, we now discuss the new technique introduced in [35] to resolve the position density $\rho := |A|^2$ from (3.5), i.e.,

$$\partial_t \rho + \nabla_x \cdot (\rho \nabla_x S) = 0. \quad (3.10)$$

Obviously, at points where physical solutions for the phase are multi-valued, the corresponding density will also become multi-valued. The new difficulty for computing the density is that it may become unbounded wherever the phase starts to become multi-valued.

We now sketch the main idea in [35] by taking the 1-dimensional Schrödinger equation as an illustration, for the multi-dimensional case we refer the readers to [34]; see also Section 4.2 below for the general case. First the scalar level set function $\phi(t, x, p)$, defined in the phase space $(x, p) \in \mathbb{R}^2$ with $p = S_x$, satisfies a linear *Liouville equation*

$$\partial_t \phi + p \phi_x - V_x \phi_p = 0. \quad (3.11)$$

This level set function initiated as $p - \partial_x S_0(x)$ forms a 1-dimensional manifold in (x, p) space.

In what follows we denote \tilde{S} and $\tilde{\rho}$ as representatives of S and ρ in the phase space, respectively, so that

$$\tilde{S}(t, x, u(t, x)) = S(t, x), \quad \tilde{\rho}(t, x, u(t, x)) = \rho(t, x).$$

Hence the WKB system (3.4)-(3.5) is shown to be rewritten in phase space as

$$\partial_t \tilde{S} + p \partial_x \tilde{S} - \partial_x V \partial_p \tilde{S} = p^2/2 - V(x), \quad (3.12)$$

$$\partial_t \tilde{\rho} + p \partial_x \tilde{\rho} - \partial_x V \partial_p \tilde{\rho} = \tilde{\rho} \frac{\partial_x \phi}{\partial_p \phi}. \quad (3.13)$$

The transport equation of phase representatives for general Hamiltonian is presented later in Lemma 4.1.

The strategy to resolve \tilde{S} is to look at the graph of the function $z = \tilde{S}(x, p, t)$ in the whole domain and project the phase value onto the manifold $\phi = 0$, as described above.

The key idea in [35] to handle the singularity in ρ caused by the coupling with ϕ in (3.13) is to use a new quantity, $f(t, x, p) := \tilde{\rho}(t, x, p)|\partial_p\phi|$, which is shown to satisfy again the Liouville equation

$$\partial_t f + p\partial_x f - \partial_x V \partial_p f = 0, \quad f(0, x, p) = \rho_0(x),$$

i.e. the concentration singularities in $\tilde{\rho}$ are cancelled out by the zeros of $\partial_p\phi$!

The combination of the level set functions ϕ and the function f enables us to compute the desired density and the velocity via the integrals

$$\bar{\rho}(x, t) = \int f(t, x, p)\delta(\phi)dp, \quad \bar{u}(x, t) = \int pf(t, x, p)\delta(\phi)dp/\bar{\rho}. \quad (3.14)$$

We shall discuss the numerical implementation for evaluating the above integrals at the end of Section 4.

4 WKB approximation

In addition to the semiclassical approximation in Schrödinger equations, geometric optics applied to high frequency wave propagation problems often leads to a weakly coupled system of a Hamilton–Jacobi equation for phase S and a transport equation for density ρ :

$$\begin{aligned} \partial_t S + H(x, \nabla S) &= 0, \quad (t, x) \in R^+ \times R^n, \\ \partial_t \rho + \nabla_x \cdot (\rho \nabla_p H(x, \nabla_x S)) &= 0. \end{aligned}$$

The phase and velocity can be solved using the level set method as presented in Section 2. Following the idea introduced for the case for semi-classical approximation, we evolve the density near the n -dimensional bi-characteristic manifold of the Hamilton–Jacobi equation, that is identified as the common zeros of n level set functions in phase space $(x, k) \in \mathbb{R}^{2n}$. These level set functions are generated from solving the Liouville equation with initial data chosen to embed the phase gradient. Simultaneously we track a new quantity $f = \tilde{\rho}(t, x, k)|\det(\nabla_k\phi)|$ by solving again the Liouville equation near the obtained zero level set $\phi = 0$ but with initial density as initial data. The multi-valued density is thus resolved by integrating f along the bi-characteristic manifold in the phase directions.

We now present a complete treatment of the WKB system by first reviewing our previous level set equations for multi-valued velocity and phases, and then develop the method for computing multi-valued density and other physical observables via solutions of the Liouville equation.

4.1 Multi-valued velocity and phase

As we argued in Section 2, the multi-valued phase gradient or velocity may be implicitly realized as the zero set of a vector level function $\phi(t, \mathbf{x}, \mathbf{p}) \in \mathbb{R}^n$, satisfying the Liouville equation

$$\partial_t \phi + \nabla_{\mathbf{p}} H \cdot \nabla_{\mathbf{x}} \phi - \nabla_{\mathbf{x}} H \cdot \nabla_{\mathbf{p}} \phi = 0, \quad (4.1)$$

subject to initial data $\phi(0, \mathbf{x}, \mathbf{p}) = \mathbf{p} - \nabla_{\mathbf{x}} S_0(x)$ or its smooth approximation. Such a zero level set represents the n -dimensional bi-characteristic manifold in phase space $(\mathbf{x}, \mathbf{p}) \in \mathbb{R}^{2n}$ and gives implicitly the multi-valued phase gradient; i.e.

$$\phi(t, \mathbf{x}, \mathbf{p}) = 0, \quad \mathbf{p} = \nabla_{\mathbf{x}} S.$$

However the phase S can not be obtained from solving the Liouville equation (4.1) since S is in general not preserved along the Hamiltonian flow. Instead, in phase space (\mathbf{x}, \mathbf{p}) the phase solves a forced transport equation

$$\partial_t \tilde{S} + \nabla_{\mathbf{p}} H \cdot \nabla_{\mathbf{x}} \tilde{S} - \nabla_{\mathbf{x}} H \cdot \nabla_{\mathbf{p}} \tilde{S} = \mathbf{p} \cdot \nabla_{\mathbf{p}} H - H. \quad (4.2)$$

This formulation was first proposed in [10] to compute multi-valued phase solutions to Hamilton-Jacobi equations, it is then followed by a projection of the obtained phase value onto the n -dimensional manifold $\phi = 0$, and thus we resolve the multi-valued phase in the physical space.

4.2 Multi-valued density

Equipped with the multi-valued phase gradient $\nabla_{\mathbf{x}} S$ realized by the zero level set of ϕ , we proceed to evaluate the multi-valued density.

In the physical space we rewrite the density equation (3.5) as

$$\partial_t \rho + \nabla_{\mathbf{p}} H \cdot \nabla_{\mathbf{x}} \rho = -\rho G \quad (4.3)$$

where

$$G := \nabla_{\mathbf{x}} \cdot \nabla_{\mathbf{p}} H(\mathbf{x}, \mathbf{p}), \quad \mathbf{p} = \nabla_{\mathbf{x}} S(t, \mathbf{x}) = \mathbf{v}(t, \mathbf{x}). \quad (4.4)$$

In order to obtain the evolution equation for density in the phase space, we need to use the bi-characteristic field as shown in the following

Lemma 4.1. Let $\tilde{w}(t, \mathbf{x}, \mathbf{p})$ be a representative of $w(t, \mathbf{x})$ in the phase space such that $\tilde{w}(t, \mathbf{x}, \mathbf{v}(t, \mathbf{x})) = w(t, \mathbf{x})$. Then

$$\partial_t \tilde{w} + \nabla_{\mathbf{p}} H \cdot \nabla_{\mathbf{x}} \tilde{w} = L \tilde{w}(t, \mathbf{x}, \mathbf{p}),$$

where

$$L := \partial_t + \nabla_{\mathbf{p}} H \cdot \nabla_{\mathbf{x}} - \nabla_{\mathbf{x}} H \cdot \nabla_{\mathbf{p}}$$

denotes the Liouville operator .

Proof. Using the fact that $\tilde{w}(t, x, \mathbf{v}(t, \mathbf{x})) = w(t, \mathbf{x})$ we have

$$\begin{aligned} \partial_t w &= \partial_t \tilde{w} + \nabla_{\mathbf{p}} \tilde{w}(t, \mathbf{x}, \mathbf{p}) \cdot \partial_t \mathbf{v}, \\ \partial_{x_j} w &= \partial_{x_j} \tilde{w} + \nabla_{\mathbf{p}} \tilde{w} \cdot \partial_{x_j} \mathbf{v}, \quad j = 1 \cdots n. \end{aligned}$$

Thus a straightforward calculation yields

$$\partial_t w + \nabla_{\mathbf{p}} H \cdot \nabla_{\mathbf{x}} w = \partial_t \tilde{w} + \nabla_{\mathbf{p}} H \cdot \nabla_{\mathbf{x}} \tilde{w} + (\partial_t \mathbf{v} + \nabla_{\mathbf{p}} H \cdot \nabla_{\mathbf{x}} \mathbf{v}) \cdot \nabla_{\mathbf{p}} \tilde{w}.$$

Differentiation of the equation $S_t + H(x, \mathbf{v}) = 0$ leads to the velocity equation

$$\partial_t \mathbf{v} + \nabla_{\mathbf{p}} H \cdot \nabla_{\mathbf{x}} \mathbf{v} = -\nabla_x H.$$

A combination of the above two equations leads to $L\tilde{w}$ as asserted. □

Based on this lemma and (4.3) we have

$$L\tilde{\rho} = -\tilde{\rho}G. \tag{4.5}$$

We still need to evaluate G , given in (4.4), in the phase space via the level set function ϕ . Let $Q := \nabla_{\mathbf{p}} \phi(t, \mathbf{x}, \mathbf{p})$, the invertibility of Q is assumed in our formal derivation. The differentiation of $\phi(t, \mathbf{x}, \mathbf{v}(t, \mathbf{x})) = 0$ gives

$$\partial_t \mathbf{v} = -Q^{-1} \partial_t \phi, \quad \partial_{x_j} \mathbf{v} = -Q^{-1} \partial_{x_j} \phi, \quad j = 1 \cdots n,$$

which used in (4.4) leads to

$$G = \sum_{j=1}^n H_{x_j k_j} - \sum_{j,l=1}^n H_{k_j k_l} (Q^{-1} \phi_{x_j})^l. \tag{4.6}$$

Following Section 3 we evaluate the multi-valued density in the physical space by projecting its value in phase space (\mathbf{x}, \mathbf{p}) onto the manifold $\phi = 0$, i.e., for any x we compute

$$\bar{\rho}(\mathbf{x}, t) = \int \tilde{\rho}(t, \mathbf{x}, \mathbf{p}) |J(t, \mathbf{x}, \mathbf{p})| \delta(\phi) d\mathbf{p},$$

where

$$J := \det(\nabla_{\mathbf{p}} \phi) = \det(Q).$$

Such a Jacobian matrix actually solves

$$L(J) = JG. \tag{4.7}$$

We shall prove this below. Combining this result with the density equation (4.5) gives us:

$$L(\tilde{\rho}(t, \mathbf{x}, \mathbf{p}) |J(t, \mathbf{x}, \mathbf{p})|) = 0.$$

This equation suggests that we just need to compute the quantity

$$f(t, \mathbf{x}, \mathbf{p}) := \tilde{\rho}(t, \mathbf{x}, \mathbf{p})|J(t, \mathbf{x}, \mathbf{p})|, \tag{4.8}$$

by solving the Liouville equation

$$\partial_t f + \nabla_{\mathbf{p}} H \cdot \nabla_{\mathbf{x}} f - \nabla_{\mathbf{x}} H \cdot \nabla_{\mathbf{p}} f = 0, \tag{4.9}$$

subject to the initial condition $f_0 = \rho_0(\mathbf{x})J_0(\mathbf{x}, \mathbf{p})$, where $J_0 = 1$ if $\phi_0 = \mathbf{p} - \nabla_{\mathbf{x}} S_0$ is smooth, and $J_0 = |\det(Q_0(\mathbf{x}, \mathbf{p}))|$ for ϕ_0 chosen otherwise. With this quantity f the singularities in density ρ are cancelled out by the zeros of $J(\phi)$! Thus we can locally compute the density and flux by integration of f and $\mathbf{p}f$ along $\{\mathbf{p} \in \mathbb{R}^n : \phi(\mathbf{x}, \mathbf{p}) = 0\}$:

$$\bar{\rho}(\mathbf{x}) = \int_{\mathbb{R}^d} f(t, \mathbf{x}, \mathbf{p})\delta(\phi(\mathbf{x}, \mathbf{p}))d\mathbf{p}, \tag{4.10}$$

where $\delta(\phi) := \prod_{i=1}^n \delta(\phi_i)$ with ϕ_i being the i^{th} component of ϕ . We now justify the claim (4.7). By taking the gradient of the Liouville equation (4.1) with respect to \mathbf{p} we obtain the following equation for $Q = \nabla_{\mathbf{p}}\phi$

$$L(Q) = \nabla_{\mathbf{p}}(L\phi) + Q\nabla_{\mathbf{p}}\nabla_{\mathbf{x}}H - \nabla_{\mathbf{x}}\phi D_{\mathbf{p}}^2 H = Q\nabla_{\mathbf{p}}\nabla_{\mathbf{x}}H - \nabla_{\mathbf{x}}\phi D_{\mathbf{p}}^2 H,$$

where the matrices $\nabla_{\mathbf{p}}\nabla_{\mathbf{x}}H := (H_{x_j k_l})$ and $D_{\mathbf{p}}^2 H := (H_{k_j k_l})$. Using the fact that for $J = \det(Q)$ the following holds [35]

$$\{\partial_t, \nabla_{\mathbf{x}, \mathbf{p}}\}J = JTr(Q^{-1}\{\partial_t, \nabla_{\mathbf{x}, \mathbf{p}}\}Q), \tag{4.11}$$

we have

$$L(J) = JTr(Q^{-1}L(Q)),$$

where Tr is the usual trace map. This implies that

$$\begin{aligned} L(J) &= JTr(Q^{-1}Q\nabla_{\mathbf{p}}\nabla_{\mathbf{x}}H - Q^{-1}\nabla_{\mathbf{x}}\phi D_{\mathbf{p}}^2 H) \\ &= J [Tr(\nabla_{\mathbf{p}}\nabla_{\mathbf{x}}H) - Tr(Q^{-1}\nabla_{\mathbf{x}}\phi D_{\mathbf{p}}^2 H)] \\ &= J \left[\sum_{j=1}^n H_{x_j k_j} - \sum_{j,l=1}^n (Q^{-1}\phi_{x_j})^l H_{k_l k_j} \right] \\ &= JG, \end{aligned}$$

as claimed in (4.7).

4.3 Optical waves

We begin with the linear scalar wave equation

$$\partial_t^2 u - c^2(\mathbf{x})\Delta u = 0, \quad (t, \mathbf{x}) \in \mathbb{R}^+ \times \mathbb{R}^n, \tag{4.12}$$

where $c(\mathbf{x})$ is the local speed of wave propagation of the medium. We complement (4.12) with highly oscillatory initial data that generate high frequency solutions. The derivation of the geometrical optics equations in the linear case is classical and performed based on the usual asymptotic WKB expansion [31],

$$u(t, \mathbf{x}) = A^\epsilon(t, \mathbf{x})e^{i\frac{S(t, \mathbf{x})}{\epsilon}} \tag{4.13}$$

with

$$A^\epsilon(t, \mathbf{x}) = \sum_{l=0}^{\infty} \epsilon^l A_l(t, \mathbf{x})i^{-l}.$$

We now substitute the expression (4.13) into (4.12) and equate coefficients of powers of ϵ to zero. For ϵ^2 , this, due to the sign ambiguity, gives two eikonal equations

$$\partial_t S \pm c(\mathbf{x})|\nabla_{\mathbf{x}} S| = 0. \tag{4.14}$$

Without loss of generality we will henceforth consider the one with a plus sign. For ϵ^1 , we get the *transport equation* for the first amplitude term,

$$\partial_t A_0 + c(\mathbf{x})\frac{\nabla_{\mathbf{x}} S \cdot \nabla_{\mathbf{x}} A_0}{|\nabla_{\mathbf{x}} S|} + \frac{c^2 \Delta S - \partial_t^2 S}{2c|\nabla_{\mathbf{x}} S|} A_0 = 0. \tag{4.15}$$

In order to use the approach introduced in Section 2, we need to further simplify this transport equation and find a quantity ρ so that both S and ρ solve the WKB system with the Hamiltonian $H(\mathbf{x}, \mathbf{p}) = c(\mathbf{x})|\mathbf{p}|$. To this end we apply the differential operator ∂_t to the eikonal equation $\partial_t S + c(\mathbf{x})|\nabla_{\mathbf{x}} S| = 0$,

$$\begin{aligned} \partial_t^2 S &= -c(\mathbf{x})\partial_t|\nabla_{\mathbf{x}} S| = -c(\mathbf{x})\frac{\nabla_{\mathbf{x}} S}{|\nabla_{\mathbf{x}} S|} \cdot \nabla_{\mathbf{x}} \partial_t S \\ &= c(\mathbf{x})\frac{\nabla_{\mathbf{x}} S}{|\nabla_{\mathbf{x}} S|} \cdot \nabla_{\mathbf{x}}(c(\mathbf{x})|\nabla_{\mathbf{x}} S|). \end{aligned}$$

This enables us to simplify the coefficient of $A_0/2$ in (4.15) as

$$\begin{aligned} \frac{c^2 \Delta S - \partial_t^2 S}{c|\nabla_{\mathbf{x}} S|} &= c\frac{\Delta S}{|\nabla_{\mathbf{x}} S|} - \frac{\nabla_{\mathbf{x}} S}{|\nabla_{\mathbf{x}} S|^2} \cdot \nabla_{\mathbf{x}}(c(\mathbf{x})|\nabla_{\mathbf{x}} S|) \\ &= \nabla_{\mathbf{x}} \cdot \left(c(\mathbf{x})\frac{\nabla_{\mathbf{x}} S}{|\nabla_{\mathbf{x}} S|} \right) - 2\nabla_{\mathbf{x}} c \cdot \frac{\nabla_{\mathbf{x}} S}{|\nabla_{\mathbf{x}} S|}. \end{aligned}$$

Thereby (4.15) can be rewritten as

$$\partial_t A_0^2 + c \frac{\nabla_{\mathbf{x}} S}{|\nabla_{\mathbf{x}} S|} \cdot \nabla_{\mathbf{x}} A_0^2 + \left(\nabla_{\mathbf{x}} \cdot \left(c(\mathbf{x}) \frac{\nabla_{\mathbf{x}} S}{|\nabla_{\mathbf{x}} S|} \right) - 2 \nabla_{\mathbf{x}} c \cdot \frac{\nabla_{\mathbf{x}} S}{|\nabla_{\mathbf{x}} S|} \right) A_0^2 = 0,$$

that is

$$\partial_t A_0^2 + c^2 \nabla_{\mathbf{x}} \cdot \left(A_0^2 \frac{\nabla_{\mathbf{x}} S}{c(\mathbf{x}) |\nabla_{\mathbf{x}} S|} \right) = 0.$$

This suggests that $\rho = A_0^2/c^2$ satisfies the conservative transport equation

$$\partial_t \rho + \nabla_{\mathbf{x}} \cdot (\rho \nabla_{\mathbf{x}} H(\mathbf{x}, \nabla_{\mathbf{x}} S)) = 0,$$

with $H(\mathbf{x}, \mathbf{p}) = c(\mathbf{x})|\mathbf{p}|$. We also note that for the eikonal equation with negative sign the weighted density A_0^2/c^2 still satisfies the above conservative transport equation except for that $H(\mathbf{x}, \mathbf{p}) = -c|\mathbf{p}|$.

4.4 Numerical methods for evaluating the amplitudes and other observables

In the level set frameworks for both semiclassical limits or WKB solutions, the density and other related physical observables are tracked by a modified scalar quantity, f , that satisfies the same Hamiltonian flow as the wave fronts. The wave fronts are represented implicitly by the zero of a system of level set functions, and the new quantity, f , is related to the density distribution and the structure of the level set system.

We summarize our algorithm for computing the amplitude \bar{A}^2 as follows.

1. Initialize: construct the level set functions $\Phi_0 = (\phi_j^{(0)})$ that embed the initial data $\nabla_{\mathbf{x}} S_0$,

$$\phi_j^{(0)}(\mathbf{x}, \mathbf{k}) = k_j - \frac{\partial}{\partial x_j} S_0(\mathbf{x}), j = 1, \dots, n,$$

and the phase space amplitude function

$$f_0(x, \mathbf{k}) = \alpha(x) \bar{A}_0^2(x),$$

Here $\mathbf{k} = (k_1, k_2, \dots, k_n)$, and $\alpha(x)$ is a function that depends on the given problem. For Schrödinger equations, $\alpha(x) \equiv 1$, and for scalar wave equations, $\alpha(x)$ is the square of the wave speed.

2. Evolve the Liouville equation in phase space using $\phi_j^{(0)}$ and f_0 constructed above as initial conditions:

$$w_t + \nabla_{\mathbf{k}} H \cdot \nabla_{\mathbf{x}} w - \nabla_{\mathbf{x}} H \cdot \nabla_{\mathbf{k}} w = 0,$$

$j = 1, \dots, n$, and f_0 respectively.

3. Evaluate $\bar{A}^2(\mathbf{x}, t)$ by integrating f along $\{\mathbf{k} \in \mathbb{R}^d : \Phi(\mathbf{x}, \mathbf{k}) = 0\}$:

$$\bar{A}^2(t, \mathbf{x}) = \int_{\mathbb{R}^d} f(t, \mathbf{x}, \mathbf{k}) \delta(\Phi(\mathbf{x}, \mathbf{k})) d\mathbf{k},$$

where $\delta(\Phi) := \prod_{j=1}^n \delta(\phi_j)$ with ϕ_j being the j -th component of Φ .

On numerical integration of ρ

We first remind the readers that in the context of WKB approximations, $\rho_h = A_0^2$. In the evaluation of the density integral

$$\bar{\rho}(x, t) = \int_{\mathbb{R}^d} f(x, p) \Pi_j \delta(\phi_j(x, p)) dp, \tag{4.16}$$

typically, one replaces the Dirac- δ distribution by an approximation δ_η , such that $\delta_\eta \rightarrow \delta$ as $\eta \rightarrow 0+$. Common choices of δ_η range from a normalized Gaussian to compactly supported kernels with $2\eta > 0$ denoting the support size. Integral (4.16) is then approximated by a Riemann sum over a uniform grid with mesh size h . For example, for $d = 2$, we have:

$$\bar{\rho}_{h,\eta}(x, t) = \sum_{i,j} h^2 f(x, p_{i,j}, t) \delta_\eta(\phi_1(x, p_{i,j}, t)) \delta_\eta(\phi_2(x, p_{i,j}, t));$$

here $\bar{\rho}$ is a function of two spatial dimensions. One concludes that

$$\bar{\rho} = \lim_{\eta \rightarrow 0+} \lim_{h \rightarrow 0+} \bar{\rho}_{h,\eta},$$

if the limits are evaluated in the order as above. However, in actual numerical computation, it is important to compute convergent approximations of (4.16) as $h \rightarrow 0$ efficiently and with good quality for a given range of grid sizes, i.e. small error relative to the grid size. A common practice is to put the amount of regularization η , here corresponding to the support size, as a function of h such that $\eta(h) \rightarrow 0+$ as $h \rightarrow 0+$. However, it is not obvious that $\rho_h = \rho_{h,\eta(h)}$ converges to $\bar{\rho}$. In our study, we found that it is essential to sample δ_η correctly over the grid. This amounts to the correct selection of the kernel δ_η and the regularization parameter η in relation to both the given grid geometry, and the gradient of the level set functions.

We use the simple piecewise linear kernel

$$\delta_\eta^{(1)}(x) = \begin{cases} \frac{1}{\eta} (1 - \frac{|x|}{\eta}), & |\frac{x}{\eta}| \leq 1 \\ 0, & |\frac{x}{\eta}| > 1 \end{cases}$$

to illustrate our reasoning. First, the delta function needs to be resolved by the grid. Let $x_j = jh$ denote the grid points. If we choose an $\eta_0(h)$ smaller than the grid size, it is obvious that $\delta_{\eta_0(h)}^{(1)}$ is equivalent to 0 on the grid, regardless of the grid size. Thus $\eta(h) \geq h$. Since the integrals of interest in this paper involve the composition of δ -function and a level set function, we need to study the scaling of the regularization under this composition. Let $\phi(x)$ be the one dimensional level set function: $\phi(x) = px, p > 0$. Let $z_j = \phi(x_j) = p \cdot jh$. We see that $\eta(h)$ has to be greater than ph in order for the discretization to take effect; i.e. the amount of regularization should be an increasing function of the magnitude of the gradient of the level set function! Special techniques are needed in order to avoid grid effects that result in $\mathcal{O}(1)$ error regardless of grid refinement. It is pointed out in [58] that

if η is chosen to be positive integer multiple of h , $\kappa_0 h$, then $\delta_\eta^{(1)}(x)$ as well as the cosine kernel

$$\delta_\eta^{(2)}(x) = \begin{cases} \frac{1}{2\eta}(1 + \cos \frac{|\pi x|}{\eta}), & |\frac{x}{\eta}| \leq 1 \\ 0, & |\frac{x}{\eta}| > 1 \end{cases}$$

have the so-called “exact integration property”, meaning

$$\sum_{j=-N}^N \delta_{\kappa_0 h}^{(k)}(x_j - x_0)h = 1, \text{ for any } -Nh < x_0 < Nh, \quad k = 1, 2.$$

We remark that not all approximate delta functions satisfy the exact integration property. Moreover, even if the kernel is chosen to be either $\delta_\eta^{(1)}$, $\delta_\eta^{(2)}$, or one with many vanishing moments, if η is chosen carelessly, one typically will get a small error that does not vanish as $h \rightarrow 0$. Our experience suggests that, in general, the scaling similar to $\eta(h) = \sqrt{h}$ should be used for convergence. To see this, consider the periodic extension of $f(x)\delta_\eta(x)$, where $\delta(x)$ is supported in $[-1, 1]$ and $\delta_\eta(x) = \delta(x/\eta)/\eta$. Furthermore, let $\mathcal{S} = \int_{\mathbb{R}} f(x)\delta(x)dx = f(0)$, $I_\eta = \int_{[-\eta, \eta]} f(x)\delta_\eta(x)dx$ and \mathcal{S}_h be the corresponding Riemann sum with mesh size h . We see that the error can be formally bounded by

$$|\mathcal{S}_h - \mathcal{S}| \leq |\mathcal{S}_h - I_\eta| + |I_\eta - \mathcal{S}|.$$

Now consider the cosine kernel, $\delta_\eta^{(2)}$, and assume that f is a smooth function. Then we know that the periodic extension of $f(x)\delta_\eta^{(2)}(x)$ is a C^2 function on \mathbb{R} , and thus the quadrature error is bounded by

$$|\mathcal{S}_h - I_\eta| \leq C_0 \eta \cdot \frac{d^2}{dx^2}(f(x)\delta_\eta^{(2)}(x)) \leq \tilde{C}_0 \frac{h^2}{\eta^2}.$$

Since $\delta_\eta^{(2)}$ has one vanishing moment, $|I_\eta - \mathcal{S}| \leq C_1 \eta^2$. Hence, by choosing $\eta = \sqrt{h}$, the optimal error bound

$$|\mathcal{S}_h - \mathcal{S}| \leq h$$

is achieved. The scaling of this kind raises the question about the quality of solution for real computations. Clearly, the \sqrt{h} -scaling on the support size implies excessive smearing with respect to the given grid configuration. Moreover, in the above context, it imposes a condition on the size of the grid; i.e. there should always be $C_0 h^{-1/2}$ grid points near the location of the point mass, x_0 . In our case, this translates to the restriction of the mesh size in relation with the diameter of each connected component of $\{p : \phi(x, p) < 0\}$ for each x .

In our simulations, we use $\delta_\eta^{(2)}(x)$ and scale η with $|\phi_p|$ by

$$\eta(h, |\phi_p|) = 2 \max(|\phi_p|, 1) \cdot h.$$

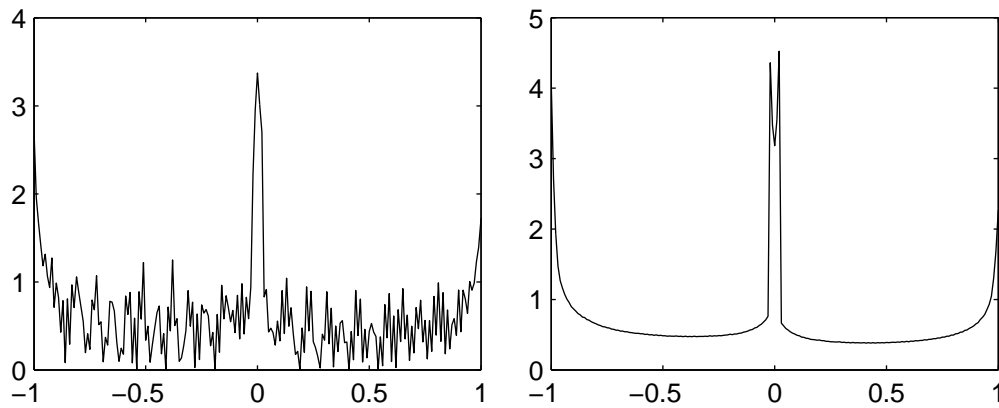


Figure 1: A numerical study of the regularization of the δ function. The plot on the left is the density obtained from using a support size that is constant multiple of the grid size. The right one is the density integral evaluated with the proposed scaling. These are numerical solutions to the problem described in Example 6.1.

Here, $|\phi_p|$ denotes the Jacobian of $\Phi = (\phi_j)$ with respect to p :

$$|\partial\Phi/\partial(p_1, \dots, p_d)|,$$

and is approximated by central differencing. Fig. 1 is a comparison using additional scaling factors. In higher dimensions ($d \geq 2$), [20] suggests the possibility of subtle complications related to the grid effects. This means that the regularization parameter η should also depend on $\nabla_{x,p}\phi_j, j = 1, \dots, d$. In our computations, we either use the same scaling as described above or perform distance reinitializations together with orthogonality adjustments on ϕ_j , as suggested in [10, 48], and recompute f due to the change in $|\partial\Phi/\partial(p_1, \dots, p_d)|$ and finally scale η as suggested.

See Fig. 1 for a comparison of the integrations computed with a “good” and a “bad” delta function.

There is, however, an additional minor numerical issue associated to the wave equations. Consider the Hamiltonian $H(\mathbf{x}, \mathbf{p}) = c(\mathbf{x})|\mathbf{p}|$ defined with a smooth, positive function $c(x)$. The corresponding wave front velocity is $\vec{v}(\mathbf{x}, \mathbf{p}) = (c(\mathbf{x})\mathbf{p}/|\mathbf{p}|, -\nabla c(x)|\mathbf{p}|)$ is not defined in the set $O_p = \{(\mathbf{x}, \mathbf{p}) \in \mathbb{R}^{2d} : |\mathbf{p}| = 0\}$. We point out that in the papers [19] and [48], for example, the location of a single wave front is tracked by the reduced Liouville equation with \mathbf{p} constrained to lie on the sphere S^d and $|\mathbf{p}|$ replaced by $1/c(\mathbf{x})$. Thus, one does not encounter this singularity. However, wave fronts in the entire computational domains are tracked simultaneously by our formalism. The singularity in the velocity field suggests that O_p should not be part of the domain and that suitable boundary conditions may have to be prescribed at $\partial O_p \subset \mathbb{R}^{2d}$. On the other hand, in the full phase space, the trajectory of a particle under this velocity field \vec{v} , starting from $(\mathbf{x}_0, \mathbf{p}_0) \notin O_p$, will never cross O_p for all time. This is due to the energy preserving property of Hamiltonian flows. Thus the computational domain $\Omega \subset \mathbb{R}^{2d}$ may safely exclude O_p . In the following calculations, we simply place a grid in \mathbb{R}^{2d} that does not intersect with O_p , and modified our discretizations for the grid points near the set O_p . The exclusion of O_p from the domain

resembles a branch cut in phase space. At the regions of ∂O_p where the characteristics are flowing into $\mathbb{R}^{2d} \setminus O_p$, we prescribe a dimension-by-dimension extension boundary condition. Let h denote the mesh size in \mathbf{k} . Near O_p , i.e. at points $(\mathbf{x}', \mathbf{k}')$ where $|\mathbf{k}'| \leq h$, if $\partial_{x_j} c(\mathbf{x}') \geq 0$, for some j , we replace backward differencing along the k_j -axis (or the corresponding WENO discretization) by forward differencing, and vice versa for the case $\partial_{x_j} c(\mathbf{x}') < 0$. This is equivalent to an extrapolation along the k_j -axis, and it somewhat resembles the Ghost Fluid method [22].

Consider the simple 1d example, in which $c(x)$ is increasing. In the upper half-plane of the $x - k$ space, the velocity is pointing in the positive x -direction and in the negative k -direction. Thus the level sets of ϕ or f will bundle up near $k = 0^+$, and the support of f may come exponentially close to the x -axis. On the other hand, in the lower half-plane, the characteristics are diverging from the x -axis. Fig. 3 illustrates this scenario. Therefore, without enforcing the boundary conditions at ∂O_p , which is the x -axis, an upwind discretization at grid points may eventually propagate portions of the energy (carried by the support of f) across the x -axis and translate it to the left! Fig. 2 shows such a situation. We point out that if \tilde{k} in Step 1 above is big enough compared to the grid and to the time interval of interest, we may not see the stated incorrect propagation of energy. Furthermore, the solution may develop a large jump across O_p and differencing across a large jump of the level set function may introduce numerical instability and may propagate portions of the energy across O , the singularity in the velocity. This potential large jump in ϕ_j and f across O_p also suggests the use of a “one-sided” approximate Dirac- δ function near O_p for better resolution of the amplitude.

A good numerical treatment of delta functions for hypersurfaces in the level set context was developed in the work of Engquist et al in [20], with the follow up work in [55], [59]. The development of the convergence theory of the delta functions concentrating on high co-dimensional geometric objects in phase space is an active area of research.

5 General symmetric hyperbolic systems

In this section we formulate the level set approach for general symmetric hyperbolic systems. The formulation in [34] is based on the derivation of the high frequency approximation using the Wigner transformation carried out in [53]. Here we describe a new derivation based on the classical method of geometric optics, see e.g. [1], and those outlined in Section 4 for the general WKB system. It again enables one to compute the higher order physical observables or moments, such as the energy and energy flux; but also enables one to compute the underlying multi-valued phase! Consider symmetric hyperbolic systems of the form

$$A(x) \frac{\partial \mathbf{u}^\epsilon}{\partial t} + \sum_{j=1}^n D^j \frac{\partial \mathbf{u}^\epsilon}{\partial x^j} = 0, \quad (5.1)$$

$$\mathbf{u}^\epsilon(0, \mathbf{x}) = \mathbf{B}_0(\mathbf{x}) e^{\frac{iS_0(\mathbf{x})}{\epsilon}}, \quad (5.2)$$

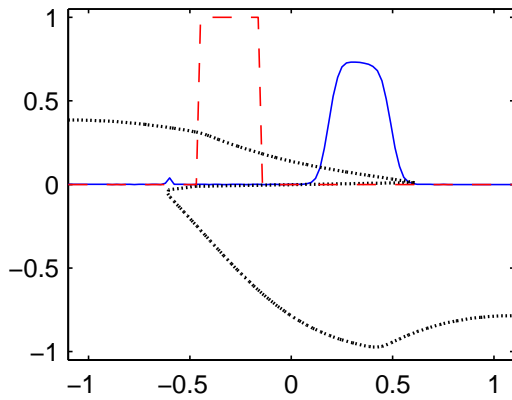


Figure 2: Inappropriate upwinding scheme incorrectly propagates an energy packet across the singularity of the velocity field in phase space. In this case, $c'(x) > 0$ and the initial phase function $S_0(x)$ is $-x^2/4$. The dashed curve represents the initial amplitude location. It is transported to the right along in the x -direction. The “ghost” energy is created and transported to the left. The dotted curve represents the computed multivalued $\nabla_x S$.

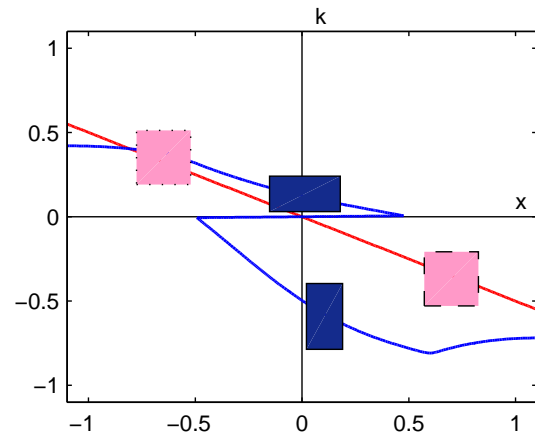


Figure 3: Illustration of the Hamiltonian flow of the optical wave equation and the transport of energy in phase space. In this case, $c'(x) > 0$ and the initial phase function $S_0(x)$ is $-x^2/4$.

where $\mathbf{u}^\epsilon \in C^M$ is a complex valued vector and $\mathbf{x} \in R^n$. Assume that the matrix $A(x)$ is symmetric and positive definite and that the matrices D^j are symmetric and independent of \mathbf{x} and t . The energy density \mathcal{E} for solution of (5.1) is given by the inner product

$$\mathcal{E}(t, \mathbf{x}) = \frac{1}{2}(A(\mathbf{x})\mathbf{u}^\epsilon(t, \mathbf{x}), \mathbf{u}^\epsilon(t, \mathbf{x})) = \frac{1}{2} \sum_{j,l=1}^n A_{jl}(\mathbf{x})u_j^\epsilon(t, \mathbf{x})\bar{u}_l^\epsilon(t, \mathbf{x}), \tag{5.3}$$

and the energy flux $\mathcal{F}(\mathbf{x})$ by

$$\mathcal{F}_j(t, \mathbf{x}) = \frac{1}{2}(D^j\mathbf{u}^\epsilon(t, \mathbf{x}), \mathbf{u}^\epsilon(t, \mathbf{x})). \tag{5.4}$$

Taking the inner product of (5.1) with $\mathbf{u}(t, \mathbf{x})$ yields the energy conservation law

$$\frac{\partial \mathcal{E}}{\partial t} + \nabla \cdot \mathcal{F} = 0. \tag{5.5}$$

Integration of (5.5) shows that the total energy is conserved:

$$\frac{\partial}{\partial t} \int \mathcal{E}(t, \mathbf{x}) d\mathbf{x} = 0. \tag{5.6}$$

Introduce the new inner product

$$\langle \mathbf{u}, \mathbf{v} \rangle_A = (A\mathbf{u}, \mathbf{v}). \tag{5.7}$$

Then the energy density is $\mathcal{E} = \frac{1}{2} \langle \mathbf{u}, \mathbf{u} \rangle_A$.

Introduce the *dispersion matrix* $L(\mathbf{x}, \mathbf{p})$

$$L(\mathbf{x}, \mathbf{p}) = A^{-1}(\mathbf{x})p_i D^i. \tag{5.8}$$

It is self-adjoint with respect to the inner product \langle, \rangle_A :

$$\langle L\mathbf{u}, \mathbf{v} \rangle_A = \langle \mathbf{u}, L\mathbf{v} \rangle_A. \tag{5.9}$$

Therefore, all its eigenvalues ω_τ are real and the corresponding eigenvectors \mathbf{b}^τ can be chosen to be orthogonal with respect to \langle, \rangle_A :

$$L(\mathbf{x}, \mathbf{p})\mathbf{b}^\tau(\mathbf{x}, \mathbf{p}) = \omega_\tau(\mathbf{x}, \mathbf{p})\mathbf{b}^\tau(\mathbf{x}, \mathbf{p}), \quad \langle \mathbf{b}^\tau, \mathbf{b}^\beta \rangle_A = \delta_{\tau\beta}. \tag{5.10}$$

We assume that the eigenvalues have constant multiplicity independent of \mathbf{x}, \mathbf{p} . This hypothesis is satisfied by many physical examples. We also assume that all the eigenvalues $\omega_\tau(\mathbf{x}, \mathbf{p})$ are simple.

Set the WKB ansatz

$$\mathbf{u}^\epsilon = e^{iS/\epsilon} \mathbf{v}^\epsilon(x, t).$$

Insertion of this ansatz into equation (5.1) leads to the following problem for \mathbf{v}^ϵ

$$\frac{i}{\epsilon} [S_t + L(x, \nabla_x S)] \mathbf{v}^\epsilon + [\partial_t + L(x, \nabla_x)] \cdot \mathbf{v}^\epsilon = 0.$$

Let $\partial_t S = -\omega_\tau$ and $\nabla_x S = \mathbf{p}$. We have the Hamilton-Jacobi equation

$$\partial_t S_\tau + \omega_\tau(x, \nabla_x S_\tau) = 0, \quad S_\tau(x, 0) = S_0(x). \tag{5.11}$$

If we fix τ and let S (subscript omitted) be obtained from this HJ equation, we can proceed to handle the amplitude

$$\mathbf{v}^\epsilon = \mathbf{v}_0 + \epsilon \mathbf{v}_1 + \epsilon^2 \mathbf{v}_2 + \dots.$$

Taking $\mathbf{v}_0 = u_0 \mathbf{b}^\tau(\nabla_x S, x)$ with u_0 to be determined, we obtain

$$\langle \mathbf{b}^\tau, [\partial_t + L(x, \nabla_x)] \cdot (u_0 \mathbf{b}^\tau) \rangle_A = 0.$$

See e.g., [1]. A straightforward calculation gives a transport equation for $\rho := |u_0|^2 = \langle v_0, v_0 \rangle_A$:

$$\partial_t \rho + \nabla_x \cdot (\rho \nabla_{\mathbf{p}} \omega_\tau(\nabla_x S, x)) = 0. \tag{5.12}$$

Applying the result in Section 4, we obtain the level set method for (5.11), (5.12) which consists of solving the following two initial value problems of the Liouville equation with bounded initial data:

$$\frac{\partial \phi^\tau}{\partial t} + \nabla_{\mathbf{p}} \omega_\tau \cdot \nabla_{\mathbf{x}} \phi^\tau - \nabla_{\mathbf{x}} \omega_\tau \cdot \nabla_{\mathbf{p}} \phi^\tau = 0, \tag{5.13}$$

$$\phi^\tau(0, \mathbf{x}, \mathbf{p}) = \phi_0^\tau(\mathbf{x}), \quad \tau = 1, \dots, n; \tag{5.14}$$

$$\frac{\partial f^\tau}{\partial t} + \nabla_{\mathbf{p}} \omega_\tau \cdot \nabla_{\mathbf{x}} f^\tau - \nabla_{\mathbf{x}} \omega_\tau \cdot \nabla_{\mathbf{p}} f^\tau = 0, \tag{5.15}$$

$$f^\tau(0, \mathbf{x}, \mathbf{p}) = \langle v_0, v_0 \rangle_A |\nabla_{\mathbf{p}} \phi_0^\tau|, \quad \tau = 1, \dots, n, \tag{5.16}$$

where $\phi_0^\tau = \mathbf{p}_\tau - \partial_{x_\tau} S_0$ for $S_0 \in C^1$, or the signed distance function otherwise. Here, assuming that ∇S_0 has simple jumps along piecewise smooth curves, we can regularize the initial data by embedding the completion of the subgraph of each component of ∇S_0 in phase space by the signed distance functions ϕ_0^τ . A similar approach to Hamilton-Jacobi equations was proposed by Giga and Sato [25]. See also [60].

Note that it follows from (4.2) that the multi-valued phase can be computed through a single-valued representative \tilde{S} in (x, p) space by solving the following linear equation

$$\partial_t \tilde{S} + \nabla_{\mathbf{p}} \omega_\tau \cdot \nabla_{\mathbf{x}} \tilde{S} - \nabla_{\mathbf{x}} \omega_\tau \cdot \nabla_{\mathbf{p}} \tilde{S} = \mathbf{p} \cdot \nabla_{\mathbf{p}} \omega_\tau - \omega_\tau. \tag{5.17}$$

Remark 5.1. In [34] we follow the Wigner transform method with projection on each eigen-mode (ω_τ, b^τ) . The scalar distribution function $a^\tau(t, \mathbf{x}, \mathbf{p})$, determined by the projection of the limit Wigner matrix

$$W^{(0)}(t, \mathbf{x}, \mathbf{p}) = \sum_{\tau=1}^n a^\tau(t, \mathbf{x}, \mathbf{p}) B^\tau(\mathbf{x}, \mathbf{p}), \quad B^\tau(\mathbf{x}, \mathbf{p}) := \mathbf{b}^\tau \mathbf{b}^{\tau*}, \tag{5.18}$$

solves the Liouville equation

$$\frac{\partial a^\tau}{\partial t} + \nabla_{\mathbf{p}} \omega_\tau \cdot \nabla_{\mathbf{x}} a^\tau - \nabla_{\mathbf{x}} \omega_\tau \cdot \nabla_{\mathbf{p}} a^\tau = 0. \tag{5.19}$$

See [53]. The initial data for a^τ is derived as

$$a^\tau(0, \mathbf{x}, \mathbf{p}) = \text{Tr}(A \mathbf{B}_0 \mathbf{B}_0^* A B^\tau) \delta(\mathbf{p} - \nabla S_0(\mathbf{x})). \tag{5.20}$$

The argument via Wigner transform is that once a^τ is computed, one can recover the Wigner matrix, and consequently the energy density and the energy flux.

The approach following the classical method of geometric optics described here is independent of the Wigner approach; and more importantly, our level set method provides a global solution

$$a^\tau(t, \mathbf{x}, \mathbf{p}) = f^\tau(t, \mathbf{x}, \mathbf{p}) \delta(\phi(t, \mathbf{x}, \mathbf{p})). \tag{5.21}$$

for the limiting Wigner equation (5.19), (5.20) when the initial amplitude $B_0 = u_0 b^\tau(\nabla_x S_0, x)$, for which one has

$$\text{Tr}(A \mathbf{B}_0 \mathbf{B}_0^* A B^\tau) = |u_0|^2 \text{Tr}(A B^\tau) = \langle \mathbf{v}_0, \mathbf{v}_0 \rangle_A.$$

Remark 5.2. For initial data with general amplitude \mathbf{B}_0 , decomposition in terms of eigenvectors $\{\mathbf{b}^\tau\}_{\tau=1}^n$ is necessary, that is,

$$\mathbf{B}_0(\mathbf{x}) = \sum_{\tau=1}^n u_0^\tau \mathbf{b}^\tau(\nabla_x S_0(x), x),$$

where $u_0^\tau = \langle \mathbf{B}_0, b^\tau \rangle_A$.

5.1 Application to acoustic waves

We will now examine the applications to acoustic wave equations. Consider the acoustic equations for the velocity and pressure disturbances \mathbf{v} and p

$$\rho(\mathbf{x})\partial_t \mathbf{v} + \nabla_{\mathbf{x}} p = 0, \quad (5.22)$$

$$\kappa(\mathbf{x})\partial_t p + \nabla_{\mathbf{x}} \cdot \mathbf{v} = 0. \quad (5.23)$$

Here ρ is the density and κ is the compressibility. With oscillatory initial data of the form

$$\mathbf{u}(0, \mathbf{x}) = \mathbf{u}_0(\mathbf{x}) \exp(iS_0(\mathbf{x})/\epsilon)$$

where $\mathbf{u} = (\mathbf{v}, p)$ and S_0 is the initial phase function, we can look for the WKB asymptotic solution

$$\mathbf{u}(t, \mathbf{x}) = A(t, \mathbf{x}, \epsilon) \exp(iS(t, \mathbf{x})/\epsilon).$$

Note that (5.22) is a symmetric hyperbolic system and the above result can be directly applied. For acoustic waves there are four wave modes, two transverse ones are non-propagating, and two longitudinal waves are propagating with speed $\pm v(x)$, where $v(x) = \frac{1}{\sqrt{\rho(\mathbf{x})\kappa(\mathbf{x})}}$.

Let $\hat{p} = (\sin \theta \cos \phi, \sin \theta \sin \phi, \cos \theta)$, the vector

$$\mathbf{b}^+(\mathbf{x}, \hat{p}) := \left(\frac{\hat{p}}{\sqrt{2\rho}}, \frac{1}{\sqrt{2\kappa}} \right),$$

and define an amplitude function \mathcal{A} in the direction of \mathbf{b}^+ as

$$A_0 = \mathcal{A}(\mathbf{x}) \mathbf{b}^+(\mathbf{x}, \nabla_{\mathbf{x}} S).$$

According to those justified above, the nonnegative function $\rho = |\mathcal{A}|^2$ satisfies

$$\partial_t \rho + \nabla_{\mathbf{x}} \cdot (\rho \nabla_p \omega(\mathbf{x}, \nabla_{\mathbf{x}} S)) = 0,$$

coupled with the eikonal equation

$$\partial_t S + \omega(\mathbf{x}, \nabla_{\mathbf{x}} S) = 0,$$

where $\omega(\mathbf{x}, \mathbf{p}) = v(x)|\mathbf{p}|$ is a single eigenvalue of the so called dispersive matrix $L(x, \mathbf{p})$ defined in (5.8). Now this problem is a particular case of the more general symmetric hyperbolic system. To evaluate the energy and energy flux one uses

$$\mathcal{E}(t, \mathbf{x}) = \int f^+(t, \mathbf{x}, \mathbf{p}) \delta(\phi^+(t, \mathbf{x}, \mathbf{p})) d\mathbf{p}, \quad (5.24)$$

$$\mathcal{F}(t, \mathbf{x}) = \int \hat{\mathbf{p}} v(\mathbf{x}) f^+(t, \mathbf{x}, \mathbf{p}) \delta(\phi^+(t, \mathbf{x}, \mathbf{p})) d\mathbf{p}, \quad (5.25)$$

where f^+ and ϕ^+ are pre-determined from the level set system with Hamiltonian $\omega(\mathbf{x}, \mathbf{p}) = v(x)|\mathbf{p}|$.

The other longitudinal wave mode is simply identified by taking $\omega(\mathbf{x}, \mathbf{p}) = -v(x)|\mathbf{p}|$. This again falls into our framework outlined in this section.

6 Numerical examples

In this section, we present a few numerical computations for Schrödinger equations and scalar wave equations, using the algorithms described above. Multivalued wave fronts (phases), densities, and amplitudes are presented together with the corresponding observables in the physical domains.

6.1 Schrödinger equations

We present calculations for the semiclassical solutions of equation (3.1) with different smooth potential functions.

Example 6.1. 1D free motion ($V = 0$).

Fig. 4 presents a computational result with the initial conditions

$$\phi_0(x) = -\sin(\pi x)|\sin(\pi x)|, \quad \rho_0(x) = \exp(-(x - 0.5)^2).$$

Notice that in Fig. 4, the averaged velocity \bar{u} is plotted against the multivalued velocity, and their values are equal wherever the system does not develop a multi-valued solution. Fig. 5 shows a progression of velocity and the corresponding density from the initial conditions $\phi_0(x) = -\alpha(\ln(\cosh(x - \beta)) + \ln(\cosh(x + \beta)))$.

Example 6.2. Consider the 1-D model with periodic potential $V(x) = \cos(2x + 0.4)$.

Fig. 6 shows a plot at a later time for this system. The initial conditions are set to

$$S_0(x) = \sin(x + 0.15),$$

$$\rho_0(x) = \frac{1}{2\sqrt{\pi}} \left[\exp\left(- (x + \pi/2)^2\right) + \exp\left(- (x - \pi/2)^2\right) \right].$$

In this figure, we also plotted the averaged velocity, and as a function of x , it has discontinuities where $\phi_p = 0$.

Example 6.3. Consider 2-D model with quadratic potential (Harmonic oscillator $V = |x|^2/2$). We set the initial conditions to be

$$S_0(x_1, x_2) = 0.6(\sin(0.4\pi x_1) - 0.1)(\sin(0.4\pi x_2) - 0.2), \quad (6.1)$$

$$\rho_0(x) = \exp(-|x|^2) + 1.0. \quad (6.2)$$

We perform the calculation in a four dimensional phase space that includes the two physical dimensions, (x, y) , and two additional dimensions, (p, q) , that embed the information of S_x and S_y . Fig. 7 shows the averaged density of the system at time $T = 6.7$. The spikes with large values correspond to the caustics developed at $T = 6.7$.

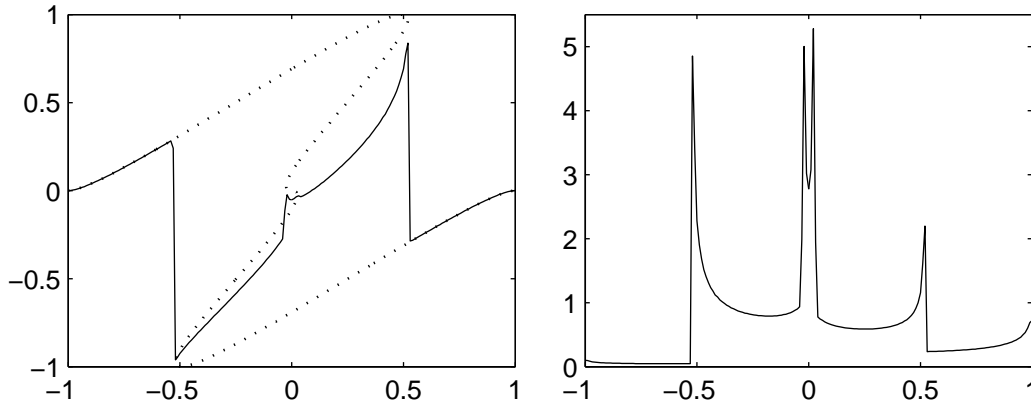


Figure 4: In the plot on the left, the multivalued velocity is shown as the dotted curve against the average velocity in solid curve. On the right is the corresponding density $\bar{\rho}$.

6.2 Scalar wave equations

This subsection presents some calculations of the wave equations (4.12). We place energy packets on a families of wave fronts (level sets of the phase S) in phase space and evolve the corresponding level set and amplitude functions. At the time when we want to evaluate the amplitude in the physical domain, a numerical integration as described in (4.16).

Example 6.4. (1D self-crossing wave fronts) $c(x) = 1.0$. $S(x) = -(x^2 - 0.25)/4$. $\bar{A}_0(x) = \chi_{[-0.7, -0.3] \cup [-.3, 0.7]}(x)$, where $\chi_\Omega(x)$ is the characteristic function of the set Ω . This simple example is designed to verify the superposition of amplitudes in linear wave propagations. We see that two groups of wave fronts each carries an amplitude of 1 is moving towards the origin. Our calculations verify that the amplitude at a given location is the addition of the amplitudes of all the wave fronts occupying the same location. See Fig. 8.

Example 6.5. (Wave guide) We are interested in a plane wave parallel to the x -axis, traveling in the positive direction in the z -axis. The index of refraction $\eta(x, y, z) = c^{-1}(x, y, z) = 1 + \exp(-x^2)$, is independent of z . In this case we can use z as time axis and reduce one more dimension. The convection in this reduced phase space, x - θ - z space, is

$$\frac{\partial}{\partial z}u + \tan \theta u_x + \frac{\eta_x}{\eta}u_\theta = 0.$$

We initialize $u(x, \theta) = \theta$, $\theta \in [-\pi/2 + \theta_0, \pi/2 - \theta_0]$, $x \in [-3, 3]$ and $f(x, \theta, z = 0) = A_0^2(x)\eta^2(x)$.

Fig. 9 shows the multivalued wave front plotted in the x - θ space (left), and

$$A^2(x, z_1) = \eta^2(x) \int f(x, \theta, z_1)\delta(\phi(x, \theta, z_1))d\theta$$

plotted as a function of x (right).

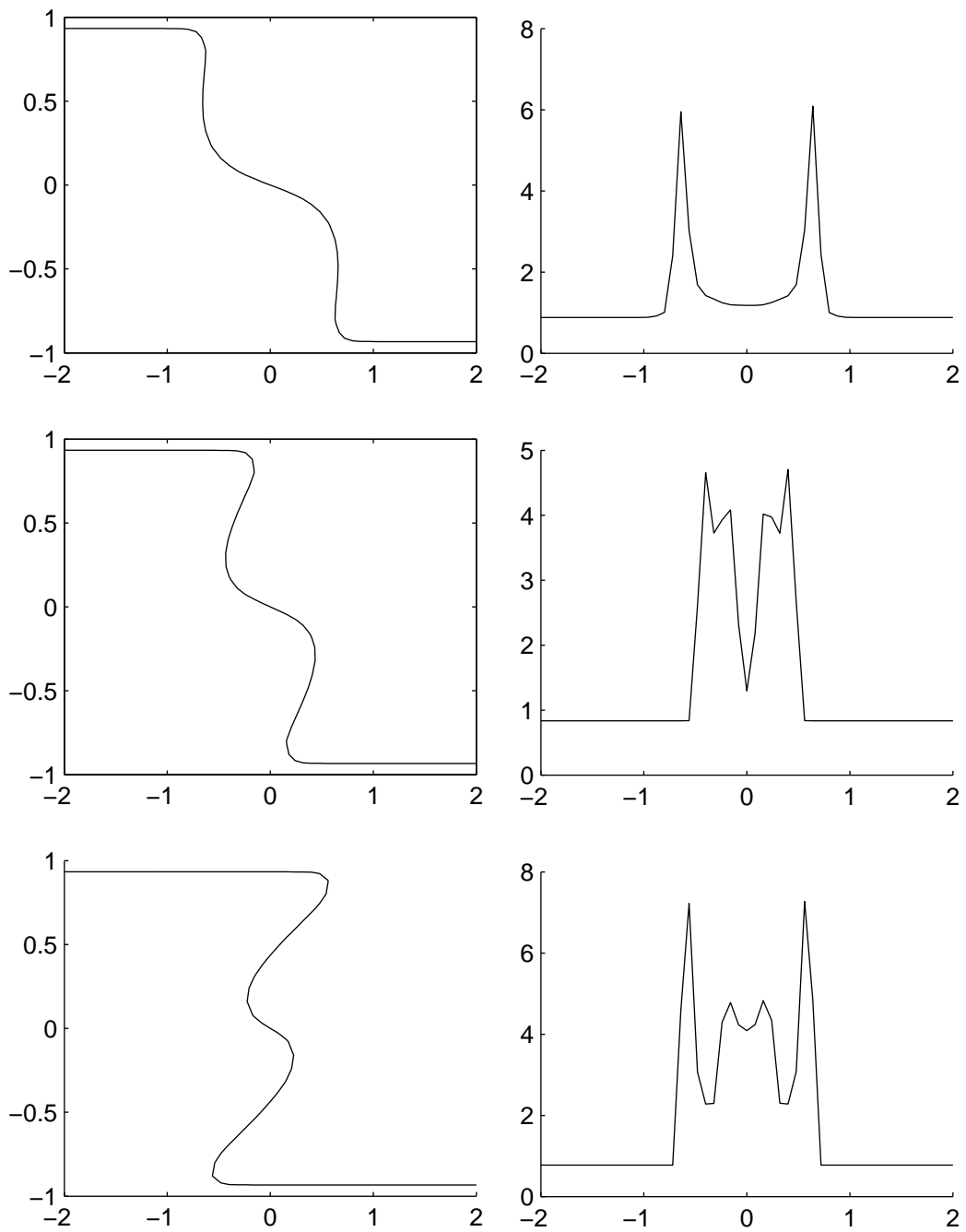


Figure 5: 5-folding in the velocity (the left column) and the corresponding averaged density (the right column). 50 grid points are used in our computation, and the results are plotted at $T = 3.5, 5.0,$ and 7.5 .

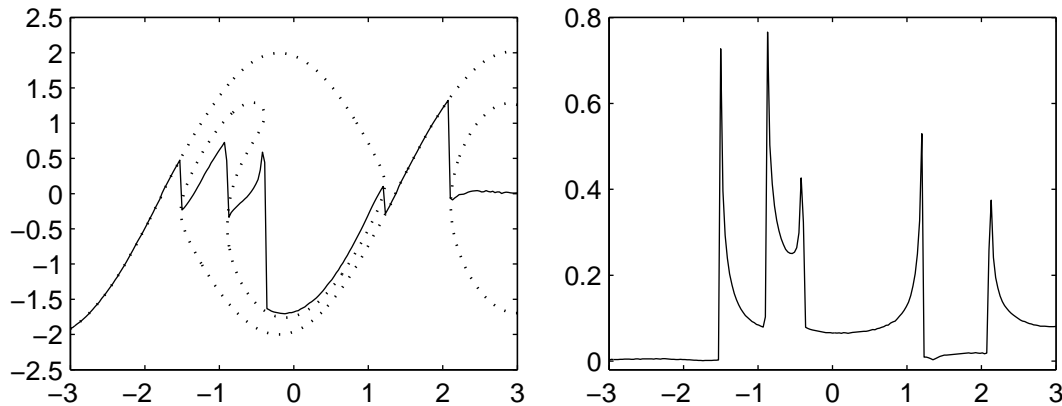


Figure 6: The dotted line and the solid line in the plot on the left correspond respectively to the multivalued phase gradient and its average (\bar{u}). The plot on the right is the corresponding density $\bar{\rho}$ at $T = 18.0$.

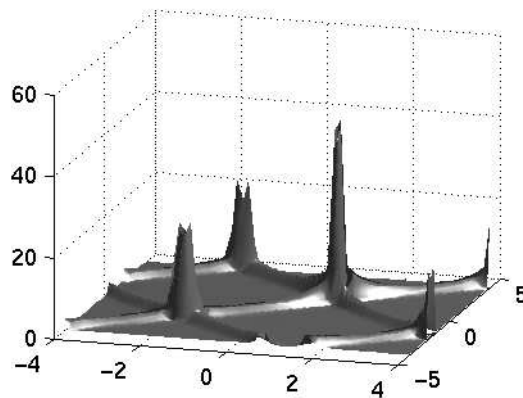


Figure 7: Averaged density of Example 6.3 at $T = 6.7$.

Example 6.6. (Contracting circle and ellipse in 2D)

Circle: $S(x, y) = -(x^2 + y^2 - 0.5)/2$, $c(x) \equiv 1$. $A_0(x, y) = 0.3 * \delta_{0.3}^{\cos}(-S(x, y))$.

Ellipse: $S(x, y) = -(x^2 + 9y^2 - 0.6)$, $c(x) \equiv 1$. $A_0(x, y) = 0.3 * \delta_{0.3}^{\cos}(-S(x, y))$.

$$\delta_{\alpha}^{\cos}(x) = \begin{cases} \frac{1}{2\alpha}(1 + \cos(\frac{\pi x}{\alpha})), & |x| \leq \eta, \\ 0, & |x| > \eta. \end{cases}$$

Figs. 10 and 11 show the respective \bar{A}^2 at different times. In addition, in Fig. 12, we plotted three wave fronts computed using raytracing on the ellipses that are initially defined by $x^2 + 9y^2 - r = 0$ with $r = 0.45, 0.6$, and 0.7 .

Example 6.7. (Waveguide) $c(x, y) = 2 - \exp(-9y^2)$, and $S_0(x, y) = x$,

$$\bar{A}_0^2(x, y) = \begin{cases} 1 & |x - 0.3| \leq 0.15, \\ 0 & \text{otherwise.} \end{cases}$$

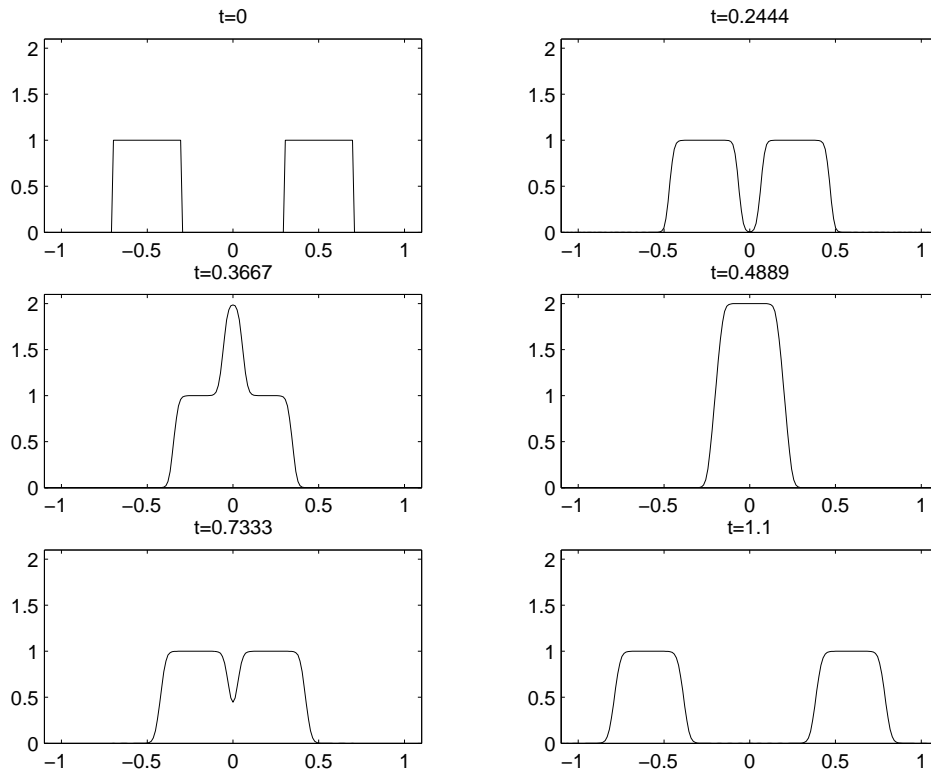


Figure 8: Self-crossing wave fronts in one dimensions.

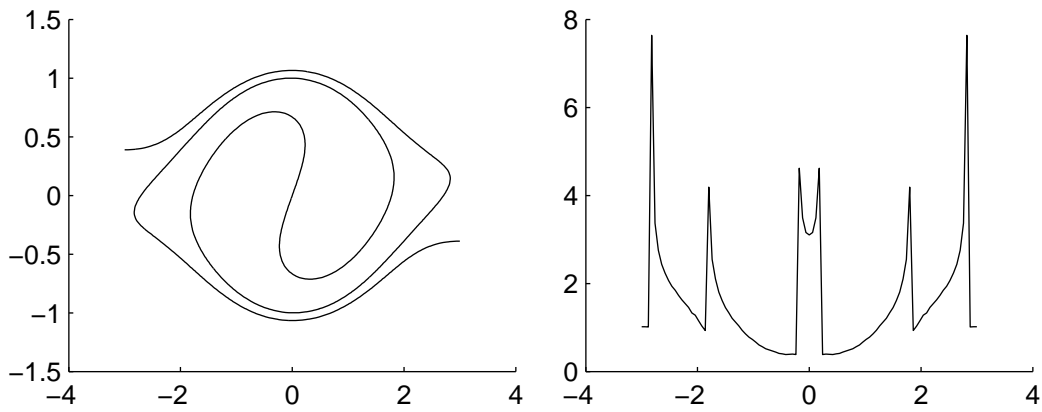


Figure 9: A multivalued wave front in a waveguide plotted in the $x - \theta$ space (left) and the corresponding amplitude, A^2 (right) .

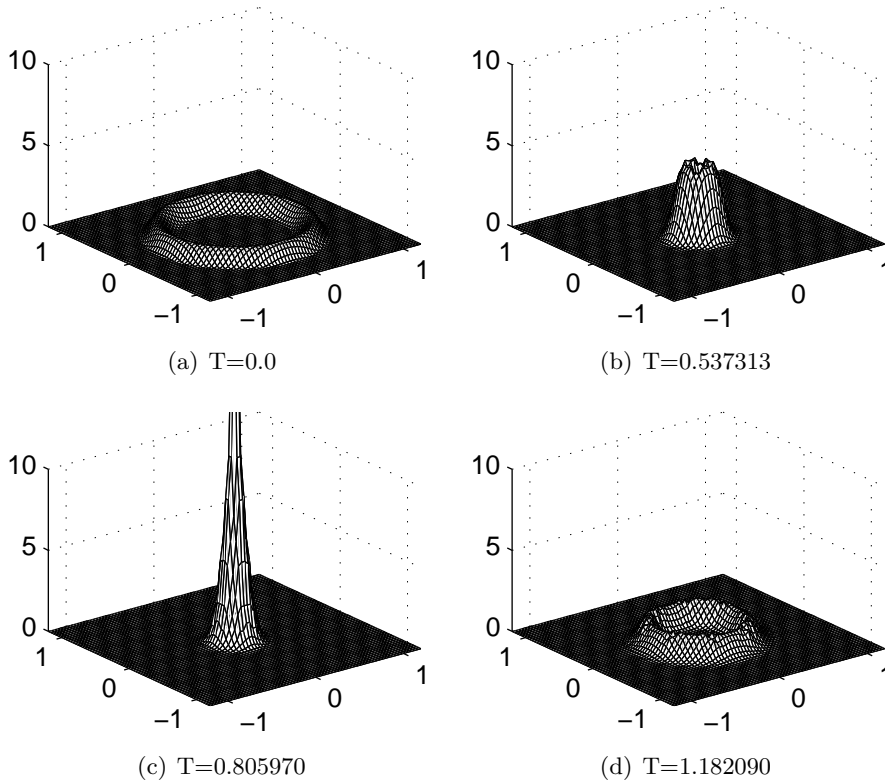


Figure 10: Contracting circle. The averaged amplitude \bar{A}^2 is plotted at different times.

Due to the slower wave speed near $y = 0$, wave fronts develop swallow tails while traveling along the x -axis towards the right. These swallow tails correspond to the formations of caustics. Fig. 13 shows four snapshots of the transport of the amplitude $\bar{A}^2(x, y, t)$. We see concentrations of energy at the corners of swallow tails.

7 Conclusions

The techniques using the level set method are naturally geometrical and very well suited for handling multi-valued solutions. Many more possibilities have yet to be explored. Future challenges lie mainly in further development of the approach to solve more real-world problems, say nonlinear wave propagation problems such as dispersive KdV equations [29], nonlinear Schrödinger equations. Recently Liu and Wang [44, 45] have introduced a field space based level set method for computing multi-valued electrical and velocity fields as well as the electron density governed by one-dimensional Euler-Poisson equations—a nonlinear system. This study suggests the possibility for developing level set methods applied to nonlinear wave propagation problems.

On the other hand, there are some analytical issues which need to be understood, such

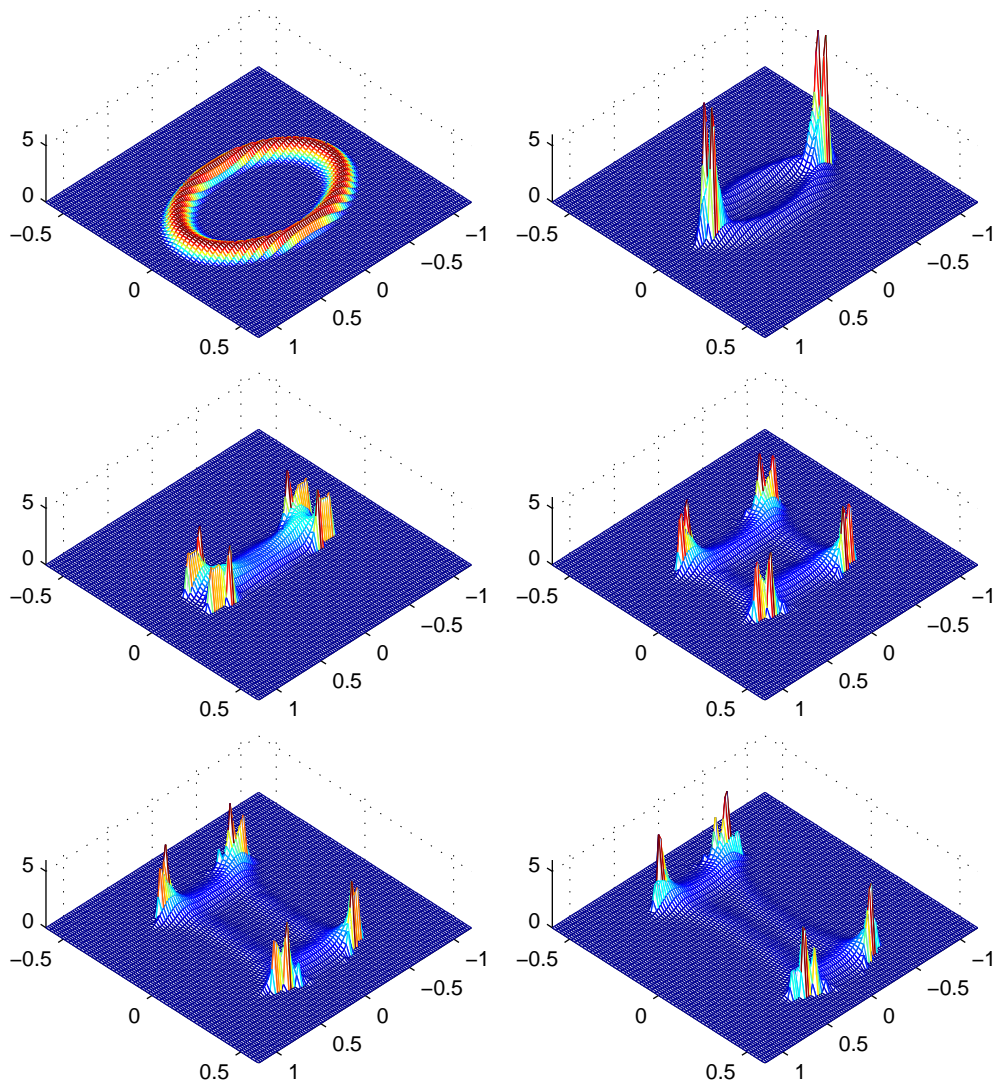


Figure 11: Contracting ellipse. The averaged amplitude \bar{A}^2 is plotted at different times (we cut off the portions of the graphs that are above 1.5).

as stability when performing geometrical operations in the augmented space and error estimates in both augmentation and projection steps. Also our understanding of how to recover original wave fields from computed observables is not completely satisfactory. Nevertheless careful numerical studies are expected to help in understanding the various issues and developing analytical results.

The solutions that are constructed by the methods mentioned in this paper are effective in the limit as the frequency goes to infinity. In many practical applications, it is important to incorporate some suitable correction so that the finite frequency nature of the problem is

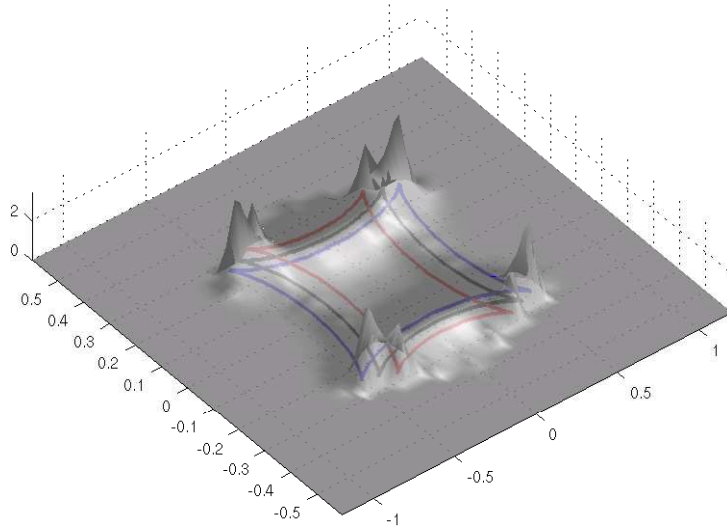


Figure 12: Contracting ellipse at $T = 0.460526$. We plotted a three wave fronts underneath the graph of \bar{A}^2 ; these wave fronts correspond to the ellipse defined, at $T = 0$, by the zeros of $x^2 + 9y^2 - r = 0$ with $r = 0.45, 0.6,$ and 0.75 .

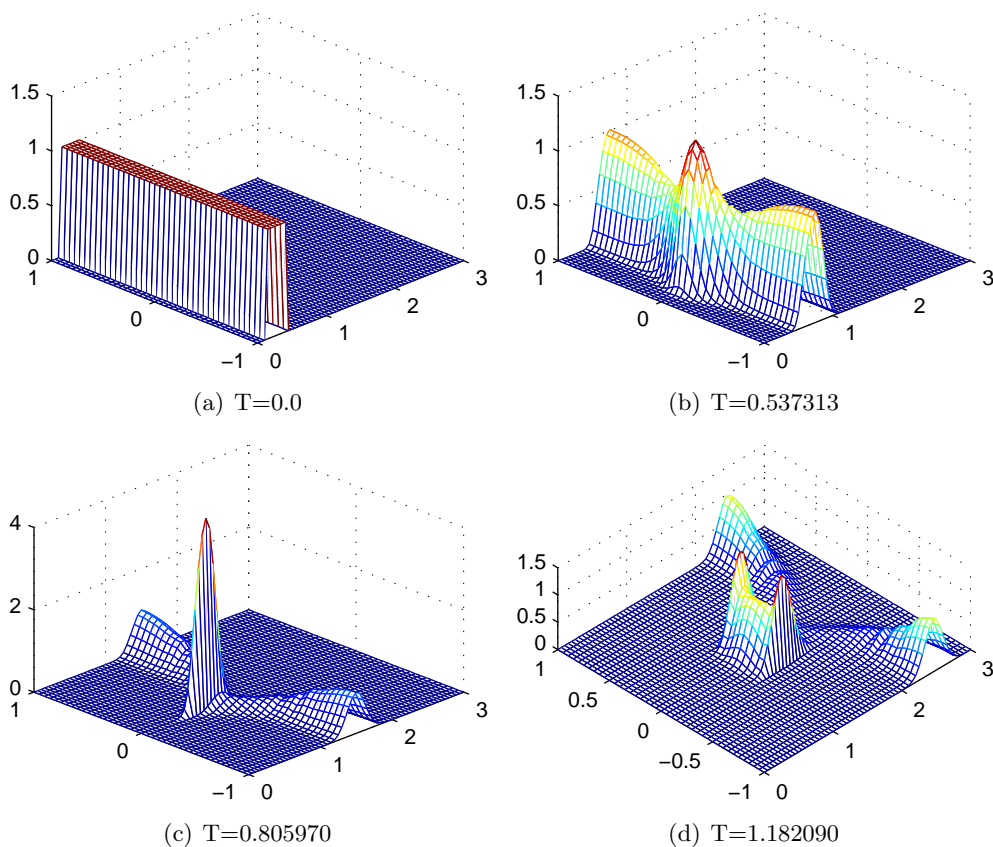


Figure 13: Multivalued wave front evolution in a waveguide.

reflected. For example, the singularities in the amplitude of the high frequency scalar wave solution is un-physical and could have important undesired consequences in solving the inverse problems in seismic imaging. Finding suitable corrections is therefore an important challenge to be resolved.

In conclusion, the results presented in this article and other results we have obtained so far show that the level set method does provide a very attractive framework for computing multi-valued solutions for nonlinear PDEs, in particular in applications to computational high frequency wave propagation problems.

Acknowledgments

In writing this review, we have drawn material from the work of many of our collaborators, including Li-Tien Cheng, Shi Jin, Jianliang Qian, and Zhongming Wang. We are very grateful to them for conversations about their recent advances that helped make this review possible. Liu's research was supported by the National Science Foundation under Grant DMS05-05975. Osher's research was supported by AFOSR Grant FA9550-04-0143. Tsai's research was supported in part by NSF DMS-0513394 and the Sloan Foundation.

References

- [1] J.L. Lions, A. Bensoussan and G. Papanicolaou, *Asymptotic Analysis for Periodic Structures*, Elsevier North-Holland, North-Holland, 1978.
- [2] J.-D. Benamou, Big ray tracing: Multi-valued travel time field computation using viscosity solutions of the eikonal equation, *J. Comput. Phys.*, 128 (1996), 463–474.
- [3] J.-D. Benamou, Direct computation of multivalued phase space solutions for Hamilton-Jacobi equations, *Commun. Pure Appl. Math.*, 52(11) (1999), 1443–1475.
- [4] F. Bouchut and F. James, Duality solutions for pressureless gases, monotone scalar conservation laws, and uniqueness, *Commun. Part. Diff. Eq.*, 24(11-12) (1999), 2173–2189.
- [5] Y. Brenier, Averaged multivalued solutions for scalar conservation laws, *SIAM J. Numer. Anal.*, 21 (1984), 1013–1037.
- [6] Y. Brenier and L. Corrias, A kinetic formulation for multi-branch entropy solutions of scalar conservation laws, *Ann. I. H. Poincaré Anal. Non-linéaire*, 15(2) (1998), 169–190.
- [7] G.-Q. Chen and H.-L. Liu, Formation of δ -shocks and vacuum states in the vanishing pressure limit of solutions to the Euler equations for isentropic fluids, *SIAM J. Math. Anal.*, 34(4) (2003), 925–938, electronic.
- [8] G.-Q. Chen and H.-L. Liu, Concentration and cavitation in solutions of the euler equations for nonisentropic fluids as the pressure vanishes, *Phys. D*, 189(1-2) (2004), 141–165.
- [9] L.-T. Cheng, *Efficient Level Set Methods for Constructing Wavefronts in Three Spatial Dimensions*, UCLA CAM Report, 2006.
- [10] L.-T. Cheng, H. Liu and S. Osher, Computational high-frequency wave propagation using the level set method, with applications to the semi-classical limit of Schrödinger equations, *Commun. Math. Sci.*, 1(3) (2003), 593–621.
- [11] L.-T. Cheng, S. Osher, M. Kang, H. Shim and Y.-H. Tsai, Reflection in a level set framework for geometric optics, *Comput. Meth. Engrg. Phys.*, 5(4) (2004), 347–360.

- [12] B. Cockburn, J. Qian, F. Reitich and J. Wang, An accurate spectral/discontinuous finite-element formulation of a phase-space-based level set approach to geometrical optics, *J. Comput. Phys.*, 208(1) (2005), 175–195.
- [13] R. Courant and D. Hilbert, *Methods of Mathematical Physics. Vol. II*, John Wiley & Sons Inc., New York, 1989. Partial Differential Equations, Reprint of the 1962 original, A Wiley-Interscience Publication.
- [14] M. Crandall and P.-L. Lions, Viscosity solutions of Hamilton-Jacobi equations, *Trans. Am. Math. Soc.*, 277(1) (1983), 1–42.
- [15] W. E, Yu. G. Rykov and Ya. G. Sinai, Generalized variational principles, global weak solutions and behavior with random initial data for systems of conservation laws arising in adhesion particle dynamics, *Commun. Math. Phys.*, 177(2) (1996), 349–380.
- [16] B. Engquist, E. Fatemi and S. Osher, Numerical resolution of the high frequency asymptotic expansion of the scalar wave equation, *J. Comput. Phys.*, 120 (1995), 145–155.
- [17] B. Engquist and O. Runborg, Multi-phase computations in geometrical optics, *J. Comput. Appl. Math.*, 74(1-2) (1996), 175–192.
- [18] B. Engquist and O. Runborg, Computational High Frequency Wave Propagation, in: *Acta Numer.*, volume 12, Cambridge University Press, Cambridge, 2003, pp. 181–266.
- [19] B. Engquist, O. Runborg and A.-K. Tornberg, High frequency wave propagation by the segment projection method, *J. Comput. Phys.*, 178(2) (2002), 373–390.
- [20] B. Engquist, A.-K. Tornberg and Y.-H. Tsai, Discretization of Dirac- δ functions in level set methods, *J. Comput. Phys.*, 207 (2005), 28-51.
- [21] L. C. Evans, A geometric interpretation of the heat equation with multivalued initial data, *SIAM J. Math. Anal.*, 27(4) (1996), 932–958.
- [22] R. Fedkiw, T. Aslam, B. Merriman and S. Osher, A non-oscillatory Eulerian approach to interfaces in multimaterial flows (the ghost fluid method), *J. Comput. Phys.*, 152 (1999), 457–492.
- [23] S. Formel and J. A. Sethian, Fast phase space computation of multiple arrivals, *Proc. Natl. Acad. Sci.*, 99(11) (2002), 7329–7334.
- [24] P. Gérard, P. A. Markowich, N. J. Mauser and F. Poupaud, Homogenization limits and Wigner transforms, *Commun. Pure Appl. Math.*, 50(4) (1997), 323–379.
- [25] Y. Giga and M.-H. Sato, A level set approach to semicontinuous viscosity solutions for Cauchy problems, *Commun. Part. Diff. Eq.*, 26(5-6) (2001), 813–839.
- [26] L. Gosse, Using K -branch entropy solutions for multivalued geometric optics computations, *J. Comput. Phys.*, 180(1) (2002), 155–182.
- [27] L. Gosse and F. James, Convergence results for an inhomogeneous system arising in various high frequency approximations, *Numer. Math.*, 90(4) (2002), 721–753.
- [28] L. Gosse, S. Jin and X. Li, On two moment systems for computing multiphase semiclassical limits of the Schrödinger equation, *Math. Mod. Meth. Appl. Sci.*, 13(12) (2003), 1689–1723.
- [29] T. Grava and F.-R. Tian, The generation, propagation, and extinction of multiphases in the KdV zero-dispersion limit, *Commun. Pure Appl. Math.*, 55(12) (2002), 1569–1639.
- [30] M. G. Forest, H. Flaschka and D. W. McLaughlin, Multi-phase averaging and the inverse spectral solution of the Korteweg-de Vries equation, *Commun. Pure Appl. Math.*, 33 (1980), 739–784.
- [31] L. Hörmander, *The Analysis of Linear Partial Differential Equations v1-4*, Springer-Verlag, Berlin, 1983-1985.
- [32] T. Katsaounis J. D. Benamou, F. Castella and B. Perthame, High-frequency Helmholtz equation, geometrical optics and particle methods, *Rev. Mat. Iberoam.*, 18 (2002), 187–209.

- [33] S. Jin and X. Li, Multi-phase computations of the semiclassical limit of the Schrödinger equation and related problems: Whitham vs Wigner, *Physica D*, 182 (2003), 46–85.
- [34] S. Jin, H.-L. Liu, S. Osher and R. Tsai, Computing multi-valued physical observables for the high frequency limit of symmetric hyperbolic systems, *J. Comput. Phys.*, 210(2) (2005), 497–518.
- [35] S. Jin, H.-L. Liu, S. Osher and Y.-H. R. Tsai, Computing multivalued physical observables for the semiclassical limit of the Schrödinger equation, *J. Comput. Phys.*, 205(1) (2005), 222–241.
- [36] S. Jin and S. Osher, A level set method for the computation of multivalued solutions to quasilinear hyperbolic PDE's and Hamilton-Jacobi equations, *Commun. Math. Sci.*, 1(3) (2003), 575–591.
- [37] S. Jin and X. Wen, Hamiltonian-preserving schemes for the Liouville equation with discontinuous potentials, *Commun. Math. Sci.*, 3(3) (2005), 285–315.
- [38] S. Jin and X. Wen, Two interface-type numerical methods for computing hyperbolic systems with geometrical source terms having concentrations, *SIAM J. Sci. Comput.*, 26(6) (2005), 2079–2101, electronic.
- [39] S. N. Kružkov, First order quasilinear equations with several independent variables, *Mat. Sb. (N.S.)*, 81(123) (1970), 228–255.
- [40] P. D. Lax and C. D. Levermore, The small dispersion limit of the Korteweg-de Vries equation. III, *Commun. Pure Appl. Math.*, 36(6) (1983), 809–829.
- [41] X. T. Li, J. G. Wöhlbier, S. Jin and J. H. Booske, Eulerian method for computing multi-valued solutions of the Euler-Poisson equations and applications to wave breaking in klystrons, *Phys. Rev. E*, 70 (2004), 016502.
- [42] P.-L. Lions and T. Paul, Sur les mesures de Wigner, *Rev. Mat. Iberoam.*, 9 (1993), 553–618.
- [43] H.-L. Liu, L.-T. Cheng and S. Osher, A level set framework for tracking multi-valued solutions to nonlinear first-order equations, *J. Sci. Comput.*, December 2005, electronic.
- [44] H.-L. Liu and Z.-M. Wang, Computing multi-valued velocity and electrical fields for 1d Euler-Poisson equations, *Appl. Numer. Math.*, to appear.
- [45] H.-L. Liu and Z.-M. Wang, A field space-based level set method for computing multi-valued solutions to 1d Euler-Poisson equations, 2006, in preparation.
- [46] C. Min, Local level set method in high dimension and codimension, *J. Comput. Phys.*, 200(1) (2004), 368–382.
- [47] S. Osher, A level set formulation for the solution of the Dirichlet problem for Hamilton-Jacobi equations, *SIAM J. Math. Anal.*, 24(5) (1993), 1145–1152.
- [48] S. Osher, L.-T. Cheng, M. Kang, H. Shim and Y.-H. Tsai, Geometric optics in a phase-space-based level set and Eulerian framework, *J. Comput. Phys.*, 179(2) (2002), 622–648.
- [49] S. Osher and R. Fedkiw, *Level Set Methods and Dynamic Implicit Surfaces*, Springer-Verlag, New York, 2002.
- [50] S. Osher and J. A. Sethian, Fronts propagating with curvature-dependent speed: Algorithms based on Hamilton-Jacobi formulations, *J. Comput. Phys.*, 79(1) (1988), 12–49.
- [51] J. Qian, L.-T. Cheng and S. Osher, A level set-based Eulerian approach for anisotropic wave propagation, *Wave Motion*, 37(4) (2003), 365–379.
- [52] J. Qian and S. Leung, A level set method for paraxial multivalued traveltimes, *J. Comput. Phys.*, 197 (2004), 711–736.
- [53] L. Ryzhik, G. Papanicolaou and J. B. Keller, Transport equations for elastic and other waves in random media, *Wave Motion*, 24(4) (1996), 327–370.
- [54] W. Sheng and T. Zhang, The Riemann problem for the transportation equations in gas dynamics, *Mem. Am. Math. Soc.*, 137(654) (1999), viii+77.

- [55] P. Smereka, The numerical approximation of a delta function with application to level set methods, *J. Comput. Phys.*, 211(1) (2006), 77–90.
- [56] C. Sparber, P.A. Markowich and N. J. Mauser, Multivalued geometrical optics: Wigner functions versus WKB-methods, *Asymptotic Anal.*, 33 (2003), 153–187.
- [57] W. Symes and J. Qian, A slowness matching Eulerian method for multivalued solutions of Eikonal equations, *J. Sci. Comput.*, 19(1-3) (2003), 501–526.
- [58] A.-K. Tornberg and B. Engquist, Regularization techniques for numerical approximation of PDEs with singularities, *J. Sci. Comput.*, 19(1-3), 2003, 527–552.
- [59] J. Towers, Two methods for discretizing a delta function supported on a level set, Preprint.
- [60] Y.-H. R. Tsai, Y. Giga and S. Osher. A level set approach for computing discontinuous solutions of Hamilton-Jacobi equations, *Math. Comp.*, 72(241) (2003), 159–181, electronic.
- [61] J. van Trier and W. W. Symes, Upwind finite-difference calculation of traveltimes, *Geophysics*, 56 (1991), 812–821.
- [62] G. B. Whitham, *Linear and Nonlinear Waves*, John Wiley & Sons Inc., New York, 1999. Reprint of the 1974 original, A Wiley-Interscience Publication.